DETECTION OF TILTED ELECTRICITY POLES USING IMAGE PROCESSING AND COMPUTER VISION TECHNIQUES

A THESIS SUBMITTED TO
THE GRADUATE SCHOOL OF NATURAL AND APPLIED SCIENCES
OF
MIDDLE EAST TECHNICAL UNIVERSITY

BY

EDİZ KARAALİ

IN PARTIAL FULFILLMENT OF THE REQUIREMENTS
FOR
THE DEGREE OF MASTER OF SCIENCE
IN
CIVIL ENGINEERING

SEPTEMBER 2023

Approval of the thesis:

DETECTION OF TILTED ELECTRICITY POLES USING IMAGE PROCESSING AND COMPUTER VISION TECHNIQUES

submitted by **EDİZ KARAALİ** in partial fulfillment of the requirements for the degree of **Master of Science in Civil Engineering, Middle East Technical University** by,

Prof. Dr. Halil Kalıpçılar
Dean, Graduate School of **Natural and Applied Sciences** _____

Prof. Dr. Erdem Canbay
Head of the Department, **Civil Engineering** _____

Assoc. Prof. Dr. Onur Pekcan
Supervisor, **Civil Engineering, METU** _____

Examining Committee Members:

Assoc. Prof. Dr. Emre Akbaş
Computer Engineering, METU _____

Assoc. Prof. Dr. Onur Pekcan
Civil Engineering, METU _____

Assoc. Prof. Dr. Seda Selçuk
Civil Engineering, Çankaya University _____

Assoc. Prof. Dr. Murat Perit Çakır
Informatics Institute, METU _____

Assoc. Prof. Dr. Hande Işık Öztürk
Civil Engineering, METU _____

Date: 04.09.2023

I hereby declare that all information in this document has been obtained and presented in accordance with academic rules and ethical conduct. I also declare that, as required by these rules and conduct, I have fully cited and referenced all material and results that are not original to this work.

Name Last name : Ediz Karaali

Signature :

ABSTRACT

DETECTION OF TILTED ELECTRICITY POLES USING IMAGE PROCESSING AND COMPUTER VISION TECHNIQUES

Karaali, Ediz
Master of Science, Civil Engineering
Supervisor: Assoc. Prof. Dr. Onur Pekcan

September 2023, 106 pages

Regular maintenance is essential in efficiently transporting electricity from one point to another to ensure an uninterrupted energy supply, and risk assessments are imperative. Since human personnel predominantly carry out such tasks, demanding a considerable workforce and causing errors, autonomous and efficient methods for effectively surveying electricity poles to detect possible anomalies are required. This study presents an autonomous risk classification model to address an anomaly type: insecurely tilted electricity poles. During this study, extensive data, 8775 electricity pole images, was gathered from various regions by Unmanned Aerial Vehicles (UAVs). An object detector, Faster R-CNN, within the proposed model was integrated to precisely identify different types of electricity poles: steel, concrete, and wooden. Subsequently, image processing techniques are deployed to determine pole tilt angles accurately. Based on these angles, electricity poles are classified as "risky" or "not risky," indicating their structural integrity and stability. The test results of the proposed model reveal the following two significant outcomes: (a) Electricity poles can be detected with a mean average precision rate of 94.40%, and (b) Representative lines for the poles and their respective tilt angles can be measured

with an accuracy of 95.95%, which demonstrates an exceptional performance. This model holds substantial promise for practically detecting risks associated with tilted electricity poles and can significantly contribute to ensuring the reliability and safety of power distribution systems.

Keywords: Tilted Pole Risk Detection, Deep Learning, Image Processing, Unmanned Aerial Vehicles, Object Detector

ÖZ

GÖRÜNTÜ İŞLEME VE DERİN ÖĞRENME TEKNİKLERİ İLE EĞİK ELEKTRİK DİREKLERİNİN TESPİTİ

Karaali, Ediz
Yüksek Lisans, İnşaat Mühendisliği
Tez Yöneticisi: Doç. Dr. Onur PEKCAN

Eylül 2023, 106 sayfa

Kesintisiz enerji tedariği sağlamak için elektriğin bir noktadan diğerine verimli bir şekilde taşınmasında düzenli bakım şarttır ve risk değerlendirmeleri zorunludur. İnsanlardan oluşan personel grubunun ağırlıklı olarak bu tür görevleri yerine getirmesi, önemli bir iş gücü gerektirmesi ve hatalara neden olması nedeniyle, elektrik direklerinin etkin bir şekilde incelenmesi ve olası anormalliklerin tespit edilmesi için otonom ve verimli yöntemler gerekmektedir. Bu çalışma, bir anormallik türünü (güvensiz şekilde eğilmiş elektrik direkleri) ele almak için otonom bir risk sınıflandırma modeli sunmaktadır. Bu çalışma sırasında İnsansız Hava Araçları (İHA) aracılığıyla çeşitli bölgelerden 8775 adet elektrik direği görüntüsünden oluşan kapsamlı bir veri toplanmıştır. Önerilen modele bir nesne tespit modeli olan Faster R-CNN entegre edilerek farklı türdeki elektrik direklerini (çelik, beton ve ahşap) kesin olarak tanımlanmıştır. Daha sonra elektrik direklerinin eğim açılarını doğru bir şekilde belirlemek için görüntü işleme teknikleri uygulanmıştır. Elektrik direkleri bu açılara göre “riskli” ve “risksiz” olarak sınıflandırılarak yapısal bütünlük ve sağlamlıklarına işaret edilir. Önerilen modelin

test sonuçları şu iki önemli sonucu ortaya koymaktadır: (a) Elektrik direkleri ortalama %94.40'lık bir ortalama hassasiyet oranıyla tespit edilebilmektedir ve (b) Direkleri temsil eden çizgiler ve ilgili eğim açıları şu şekilde ölçülebilmektedir: yüksek bir performans sergileyen %95.95'lik bir doğruluk. Bu model, eğik elektrik direkleriyle ilişkili risklerin pratik olarak tespit edilmesi konusunda umut vaat etmekte ve güç dağıtım sistemlerinin güvenilirliğinin ve emniyetinin sağlanmasına önemli ölçüde katkıda bulunabilmesi öngörülmektedir.

Anahtar Kelimeler: Eğik Direk Risk Tespiti, Derin Öğrenme, Görüntü İşleme, İnsansız Hava Araçları, Nesne Tespiti

Dedicated to my beloved family ..

ACKNOWLEDGMENTS

I would like to express my deepest gratitude to my supervisor Assoc. Prof. Dr. Onur Pekcan for his guidance, advice, patience, and encouragement during my research. He believed I could enhance my abilities, affording me a valuable opportunity. Thanks to his unwavering support, I was able to embark upon the initial stages of pursuing numerous aspirations that I had long yearned to actualize.

I would like to thank the examining committee members for being judge members for my thesis defense and examining my research.

I would like to thank my dear friends İrem Devrim, Ceren Çakmak, Ceren Genek, Melis Gizem Halli, Gülçin Gülletutan, Furkan Aydoğan, Evrim Devrim, Neşe Sarıcalı, Dila Mursaloğlu, Zeynep Zontur, Su Akavioğlu, Uygar Harputluoğlu and Begüm Mursaloğlu for their constant support and belief during my thesis study.

I would like to thank Enerjisa Energy for allowing data collection in the scope of VIS-INSPECT: Detection of the Anomalies in Energy Transmission Lines Project (No: 2020–83).

In the end, I would like to thank my dear family. They were with me at every moment and supported me in every way. If it weren't for their belief and patience, I wouldn't have been able to come to where I am now. Therefore, this thesis is dedicated to them, my mother, Hatice Karaali, my brother Zeki Karaali, and my father Selahattin Karaali.

TABLE OF CONTENTS

ABSTRACT v

ÖZ vii

ACKNOWLEDGMENTS x

TABLE OF CONTENTS xi

LIST OF TABLES xiv

LIST OF FIGURES xv

LIST OF ABBREVIATIONS xviii

CHAPTERS

1 INTRODUCTION 1

1.1 Overview and Problem Statement 1

1.2 Objectives of the Research 6

1.3 Scope of the Thesis 8

1.4 Thesis Organization 9

2 LITERATURE REVIEW 11

2.1 Data Collection Methods 12

2.1.1 Conventional Methods 12

2.1.2 Semi-automated Methods: 14

2.2 Data Processing Techniques 17

2.2.1 Research on Detection of Electricity Pole by Deep Learning Methods 18
2.2.2 Detection of Tilted Electricity Poles by Image Processing and/or Deep Learning Methods 22
2.3 Gaps in the Literature 27
3 METHOD OF TILTED ELECTRICITY POLES DETECTION 31
3.1 Object Detection Algorithms: 34
3.1.1 Image Labeling Procedure 35
3.1.2 Object Detector 36
3.1.2.1. Resnet-50 40
3.1.2.2. Feature Pyramid Networks 43
3.2 Advanced Image Processing Techniques 48
3.2.1 Converting RGB image to Grayscale image 49
3.2.2 Applying Gaussian Blur 50
3.2.3 Applying Morphological Operations 51
3.2.4 Canny Edge Detection Model 52
3.2.5 Applying Line Segment Detector 52
3.2.6 Filtering the Detected Lines According to Its Length 53
3.2.7 Extracting the Edges by Thresholding 53
3.2.8 Applying Hough Line Transform 54
3.2.9 Finding the Best Line That Represents the Electricity Poles 55
3.2.10 Measurement of the Tilt Angles of the Poles 55
3.3 Measurement of Performance Metrics 56
3.4 Risk Classification Method 57
4 FIELD EXPERIMENTS 59
4.1 Object Detection Model 63
4.1.1 Transfer Learning Method 64

4.1.2 Augmentation Techniques 65
4.1.3 Hyperparameters 66
4.1.4 Performance Metrics 66
4.1.5 Training Object Detection Model 67
4.2 Image Processing Algorithms 74
4.2.1 Validation of the Representative Lines 82
4.3 Risk Classification 83
4.4 Results and Discussion 86
5 SUMMARY, CONCLUSIONS, AND FUTURE WORK 93
5.1. Summary 93
5.2. Conclusions 94
5.3. Future Work 96
REFERENCES 99

LIST OF TABLES

TABLES

Table 1. Comparison of UAV types (Matikainen et al., 2016 & Mohsan et al., 2023 & Z. Li et al., 2011) 17
Table 2. Other Properties of DJI Mavic Pro 2 (DJI, 2023) 61
Table 3. Hyperparameters and their proposed values 66
Table 4. Description of the performance metrics' terms 67
Table 5. Detection results of the proposed object detector 70
Table 6. Results of the Performance Metrics 83

LIST OF FIGURES

FIGURES

Figure 1. Hazardously Tilted Electricity Pole 2
Figure 2. Control and Repairment Cycle for an Electricity Pole 5
Figure 3. Representation of the Proposed Model 8
Figure 4. Climbing Robots over a Power Line 13
Figure 5. Types of UAVs (a) Fixed-wing, (b) Rotary-wing (Helicopter), (c) Rotary-wing (Multi-copter) (Mohsan et al., 2023 & Stewart et al., 2021) 16
Figure 6. Results of the Object Detection Algorithm (Lin et al., 2017) 19
Figure 7. Steps of the Proposed Model (Nguyen et al., 2019b) 20
Figure 8. Detection of Electricity Tower 21
Figure 9. Classification of Towers 22
Figure 10. Architecture of the Proposed Method (Varghese et al., 2017) 23
Figure 11. Simulated images representing (a) Upright pole, (b) Fallen pole (Chen & Miao, 2019) 24
Figure 12. ROI in the Middle of an Image (Chen & Miao, 2019) 25
Figure 13. Representative architecture for the proposed model 25
Figure 14. Architecture of the Destruction Estimator Model 26
Figure 15. Representation of the Shadows and Geometric Centerlines of Towers (L. Li et al., 2021) 27
Figure 16. Comparison of Natural Inclination of Pole Types (a) Concrete Pole without Natural Structural Inclination (b) Wooden Pole without Natural Structural Inclination (c) Steel Pole with Natural Structural Inclination 33
Figure 17. Flowchart of the Proposed Risk Classification Method 34
Figure 18. Concrete, Steel, and Wooden Electricity Pole Images 36
Figure 19. Representation of Transfer Learning Method 38
Figure 20. Representative Architecture of Faster R-CNN (Ren et al., 2015) 39
Figure 21. A representation of a deep neural network (Tan & Lim, 2019) 40

Figure 22. Comparison of Two Neural Networks with Different Number of Layers (He et al., 2016b) 41
Figure 23. Representation of a Residual Block in ResNet (He et al., 2016b) 42
Figure 24. Representative Artificial Neural Network (ANN) 43
Figure 25. Representation of a Convolution Process (Zhang et al., 2018b) 45
Figure 26. Representation of a Pooling Process (Zhang et al., 2018b) 46
Figure 27. Feature Pyramid Network Architecture (Lin, Dollár, et al., 2017) 47
Figure 28. Cropping of the Bounding Box Coordination 48
Figure 29. Representation from RGB Image to Grayscale Image 49
Figure 30. Polar Coordinate System 54
Figure 31. Representative Line and Vertical Boundary of the Image 55
Figure 32. Representative Input Images for (a) Steel Pole, (b) Wooden Pole 57
Figure 33. UAV Shooting Angles from Top View 59
Figure 34. Sample Images Collected from the Test Region 60
Figure 35. Approximate Altitude of UAVs Image Shooting 62
Figure 36. Sample Application of Random Flip 65
Figure 37. The Loss Curves of Faster R-CNN Object Detector (a) Separate losses and (b) Total loss 69
Figure 38. Precision-Recall Curves (a) Classwise (b) Average Precision 71
Figure 39. Output Image Samples of the Object Detector 73
Figure 40. Converting Cropped Images to Grayscale 75
Figure 41. Applying Gaussian Blur to Input Grayscale Images 76
Figure 42. Applying Morphological Operations to Input Images 77
Figure 43. Applying Canny Edge Detector to Input Images 78
Figure 44. Representation of Extracted Edges 79
Figure 45. Proposed Lines by Hough Line Transformation 80
Figure 46. Selecting the Best Line 81
Figure 47. Example Measurement of Tilt Angle 82
Figure 48. Risk Classification Results of the Electricity Poles (a) Concrete Pole, (b) Steel Pole and (c) Wooden Pole 84

Figure 49. Output Images from The Proposed Model 85
Figure 50. Images Including Various Types of Environmental Objects..... 87
Figure 51. Images Collected for the Detection of Tilted Electricity Poles 88
Figure 52. Incorrectly Classified Wooden Pole 89
Figure 53. Images Including Shadows of the Electricity Poles 89
Figure 54. Misidentified Lines (a) Electricity Cable, and (b) Road Markings 91

LIST OF ABBREVIATIONS

ABBREVIATIONS

AI	Artificial Intelligence
ANN	Artificial Neural Network
AP	Average Precision
CNN	Convolutional Neural Network
CV	Computer Vision
EMD	Earth Mover's Distance
FPN	Feature Pyramid Network
GPS	Global Positioning System
HOG	Histograms of Oriented Gradients
IoU	Intersection of Union
LSD	Line Segment Detector
MLP	Multilayer Perceptron
RPN	Region Proposal Network
ROI	Region of Interest
SSM	Single Shot Multibox
YOLO	You Look Only Ones
UAV	Unmanned Aerial Vehicles

CHAPTER 1

INTRODUCTION

Technological advancements enable human beings to enrich their horizons to enhance and strengthen their skills in solving challenging problems. More practical and efficient solutions to real-life situations can be discovered with increasing applications of Artificial Intelligence. In this study, a real-life issue, the detection of insecurely tilted electricity poles, is investigated using computer vision and advanced image processing techniques.

1.1 Overview and Problem Statement

A sustainable electricity supply is necessary, and it is gaining even greater significance in light of the global population growth trends and urbanization. The escalating demand for electricity is related to the expanding global population, compelling energy distribution companies to allocate substantial resources towards developing and maintaining transmission infrastructure. Consequently, the significant investments made in this domain necessitate an extensive network of transmission lines spanning both urban and rural areas, requiring the implementation of efficient management and maintenance protocols (Li et al., 2014).

The significance of electricity distribution is as crucial as distributing this energy to the desired destinations. Consequently, electricity distribution companies endeavor to transmit electricity through highly efficient and complex network systems. These grid systems are instrumental in facilitating the delivery of electrical energy to consumers across vast distances, spanning hundreds of thousands of kilometers, as documented by the U.S. Energy Information Administration (EIA) in 2010.

These extensive long grid systems are classified into two primary types: local and global networks. Local grids are designed to compensate for the distribution needs of small cities, buildings, retail establishments, and businesses providing localized access to electricity. In contrast, global networks consist of multiple local grids, thereby providing a pivotal mechanism for facilitating electricity transmission over significantly extended distances. The main objective of this grid system is to establish reliable and durable electricity transmission to meet the customer's energy requirements.

While electricity distribution companies aim to distribute energy to their customers with efficient and reliable methods, it is imperative to acknowledge the presence of external factors, i.e., anomalies that can potentially result in short-term or long-term power interruptions. During this study, one of the most prevalent anomalies, hazardously tilted electricity poles, is studied (Figure 1).



Figure 1. Hazardously Tilted Electricity Pole

Tilted electricity poles are significantly correlated with the structural integrity and reliability of electricity poles, and they serve as the primary focus of this research. The tilting of electricity poles is predominantly attributed to the loss of equilibrium in suspension supports or increased tension in end supports (Malhara & Vittal, 2009).

Internal and external factors responsible for this loss of equilibrium, making these electricity poles susceptible to bending or inclination, encompass a range of influences (Yang et al., 2022):

- Unstable force transmitted through the wires
- Extreme weather conditions
- Being near the end of its operational life

Massive rainfall or wind-loading events have the potential to disrupt the stable transmission of forces along electricity cables. This phenomenon constitutes the primary factor responsible for the highly variable amplitude of vibrations during electricity transmission procedures, thereby giving rise to critical structural serviceability issues that may result in the inclination of electricity poles (Jafari et al., 2020).

Furthermore, adverse weather conditions, including severe storms, floods, and landslides, can harm electricity poles' geotechnical and structural integrity. Consequently, these conditions can impede the practical functionality of energy transmission through electricity poles (Yang et al., 2022).

In addition to the abovementioned external factors, it is imperative to recognize that each electricity pole possesses a distinct operational life. As a result, the absence of periodic maintenance and surveillance operations for the electricity corridors can culminate in structural concerns, such as the inclination of the electricity poles.

The last factor that holds the potential to impact the structural stability of electricity poles pertains to geotechnical considerations. Since all structures rely on foundations anchored within soil layers, the durability and reliability of the foundation designs for electricity poles assume great significance. Consequently, meticulous attention is imperative during the construction phase of electricity poles.

These natural and human-induced factors may result in:

- Suspension of electricity lines abnormally
- Security vulnerability around the electricity poles

Electric distribution companies are conducting surveillance and maintenance activities to mitigate or eradicate the problems associated with the electricity poles. Within these initiatives, a critical control and repair cycle has been instituted to address potential anomalies about electricity poles. This cycle consists of the following stages: (i) Conducting patrols along electricity line corridors to identify potential anomalies, (ii) Determining the types of anomalies and assessing their severity, and (iii) Repair operations for electricity poles exhibiting anomalies.

This cycle has been systematically implemented across all electricity pole corridors by electricity distribution companies using manual investigative techniques. These manual procedures are contingent upon human labor and primarily encompass the following steps (Figure 2):

I. The initial inspection entails traversing the line corridors using vehicles and visually assessing electricity poles without specialized equipment.
II. A grading or severity assessment of potential anomalies is performed. This assessment aids in classifying the abnormalities by their level of severity.
III. Finally, based on the outcomes of the severity assessment, requisite repair measures are executed.

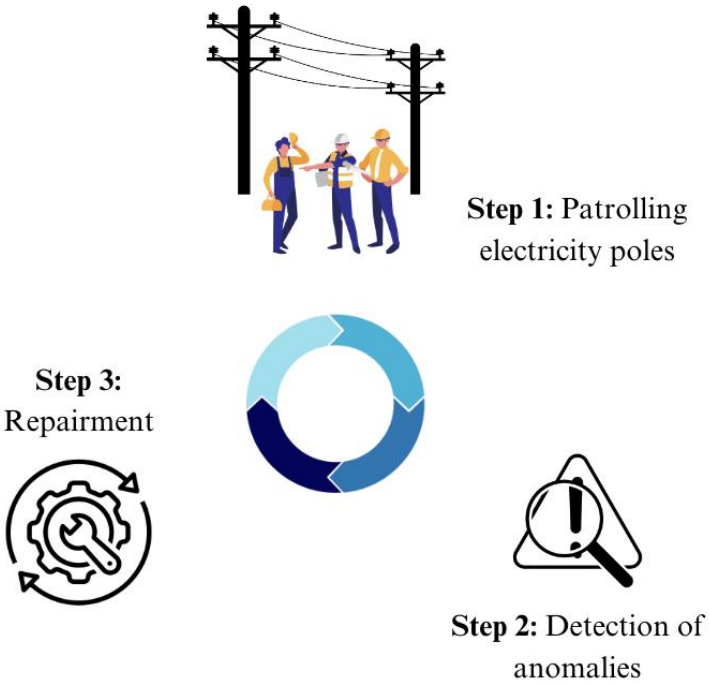

Figure 2. Control and Repairment Cycle for an Electricity Pole

As this cycle necessitates application across expansive grids spanning thousands of kilometers, several pivotal factors assume great importance. These factors include the efficiency of surveillance efforts, the precision value of anomaly detection, the extent of reliance on human labor, and the cost-effectiveness of repair solutions. Considering these factors, this study proposes an automated risk detection and classification system for inclined electricity poles. This system utilizes the capabilities of Artificial Intelligence applications, image processing techniques, and UAVs to enhance the accuracy and efficiency of anomaly assessment and management.

Throughout this study, the principal objective is tilted electricity pole detection. Consequently, in addition to diminishing the time required for identifying instances of damage and malfunction, enhancing the accuracy rate in anomaly detection is also targeted. Shortening the damage and malfunction detection time is anticipated to reduce response time, enabling continuous energy transmission to the customers.

1.2 Objectives of the Research

The principal aim of this study is to enhance an automated risk classification system, with a specific focus on detecting inclined electricity poles and conducting a comprehensive analysis of their risk status based on the quantification of their inclination angle values. As a result, it is imperative to employ proficient methods for the collection and processing of data. As a result, the main objectives of this research study will be as follows:

- One of the most efficient and expeditious approaches, UAVs, was used for high-resolution data collection. These vehicles aim to capture real electricity pole images from a level higher than the poles' height with pre-determined image shooting angles.
- Collecting electricity pole images from diverse regions, such as Ankara, Bartın, Kastamonu, and Zonguldak, facilitates the creation of a comprehensive image dataset encompassing various pole types (steel, concrete, and wooden poles), environmental conditions, and associated anomalies.
- During the risk classification method, a supervised learning approach has been employed. Consequently, a systematic labeling procedure for detecting pole types and their respective locations within the images has been carried out. This process has been facilitated through the utilization of in-house labeling software.
- An object detection model, Faster R-CNN, is utilized for training with the labeled dataset to detect the approximate positions of electricity poles within the images. This phase aims at enhancing the precision and efficiency of the object detection model.
- After detecting the locations of electricity poles within the images, these poles are cropped from the images to be employed within a sequence of image-processing techniques. The cropping procedures aim to eliminate the environmental noises around the electricity pole, and the proposed image-

processing algorithms include blurring, morphological operations, edge detection, line segment detection, and the Hough transformation to identify a representative line corresponding to the electricity poles.

- The detected representative lines are validated using two performance metrics to measure the similarity of the two lines. A separate image labeling procedure was conducted to draw the electricity poles' truth lines. After this, truth and representative lines are utilized to measure the similarity ratio of these two lines.
- After validation of the representative line for electricity poles, the primary objective is to measure the inclination angle of these poles by applying geometric principles. These principles involve the measurement of the angle between the representative line and a hypothetical vertical line.
- The quantified tilt angle is a pivotal factor in determining the risk status of electricity poles. During this procedure, the pole types identified through the proposed object detection method are utilized to establish specific allowable inclination limits. These predefined limits classify electricity poles as either 'risky' or 'not risky'.
- At the final stage of this study, the performance of the enhanced risk classification model has been subjected to rigorous examination through the utilization of a dataset gathered from a pilot test region. This evaluation has been applied to validate the effectiveness and robustness of the proposed methodology.
- Based on the above objectives, the schematic representation of the proposed risk classification system for the tilted electricity poles is provided in Figure 3.

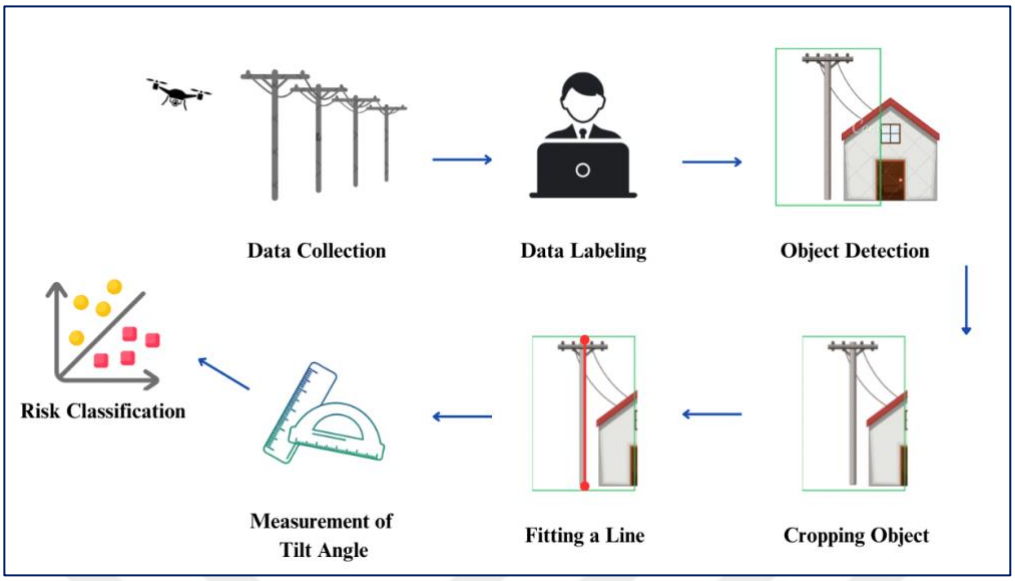

Figure 3. Representation of the Proposed Model

1.3 Scope of the Thesis

This study introduces an automated risk classification method to detect and classify tilted electricity poles. The research involves the labeling, image-processing, and testing of images acquired through UAVs. The proposed method demonstrates the capability to detect and classify three distinct types of electricity poles: (i) steel, (ii) concrete, and (iii) wooden poles, thereby expanding the versatility and applicability of the model.

The proposed model can automatically detect electricity poles, quantifying the degree of inclination for various pole types and classifying their risk status based on their tilt angles without manual patrolling procedures. This model eliminates the necessity for surveillance operations involving personnel traversing electricity line corridors and visually inspecting pole risk status. While various data collection methods exist, from portable cameras to UAVs equipped with laser scanners, conventional UAVs were selected for use in this study due to their viability, efficiency, and expeditious data collection capabilities.

1.4 Thesis Organization

This study consists of five chapters, each serving distinct purposes, with the overarching goal of explaining the data collection methods, the prior literature research, the proposed autonomous risk classification method, and presenting its results, accompanied by recommendations for future research works. Chapter 2 delves into a detailed review of the existing literature, encompassing data collection methods, object detection models, and the detection of tilted electricity poles. Chapter 3 explains the risk detection methodology, including the properties of deep learning models, their architectural specifications, and the sequential application of image processing techniques. Chapter 4 conducts a comprehensive discussion, covering the results obtained from the proposed model and performance metric values related to both the object detection and risk classification models. Additionally, a field study conducted in Polatlı, Ankara, tests the proposed method's efficacy. The concluding chapter synthesizes the proposed techniques and outlines potential directions for future research initiatives.

CHAPTER 2

LITERATURE REVIEW

Regular anomaly detection on electricity poles is one of the crucial processes for sustainable electricity transmission systems. Some frequent anomalies or damages can be observed on these systems, such as foreign objects (bird's nests, balloons, and kites) standing on the electricity poles, corrosion on the steel poles, fractures on insulators, contact of trees with electrical cables and tilted poles. Since these anomalies can cause long-term energy loss and dissatisfaction among electricity users, periodic surveillance and maintenance operations should be conducted.

Until the last 20 years, manual inspection methods were mainly utilized through the electric lines spreading over extensive regions. These manual methods are prone to a vast workforce working on the sites. According to the Turkish Electricity Transmission Corporation (2023), Turkey's total length of electricity lines is 73,806 kilometers. As a result, a considerable amount of seasoned site workers are required so that proper and confidential power line inspections can be conducted.

The rapid progression of technological advancements over the past decade has afforded electricity distribution entities alternative approaches to mitigate excessive time consumption and the imperative for substantial workforce engagement in the execution of maintenance and surveillance undertakings. These alternative methods can collect data from several distant sites by utilizing enhanced robots such as UAVs. Autonomous anomaly inspection and data collection methods with a much smaller workforce emerged thanks to UAVs. After the data collection process in autonomous systems, the gathered data are utilized for consecutive deep learning models and

image processing techniques. This chapter presents the literature studies of data collection methods and data processing techniques within the above context.

2.1 Data Collection Methods

The expansion of electricity infrastructure has necessitated the establishment of extensive transmission lines spanning thousands of kilometers across diverse locations, including cities, villages, and towns. Given these regions' distinctive characteristics and susceptibility to expansion due to the increasing demands for electricity, expeditious and precise data collection techniques become crucial. Two principal methodologies emerge for acquiring data from these varied areas: conventional and semi-automated. Traditional methods mainly include ground inspections conducted by site workers and climbing robots that travel through the power lines at relatively slower speeds. In contrast, semi-automated data collection techniques include more contemporary methods such as airspace inspection and remote sensing (Liu et al., 2020). Although both inspection methods aim to gather high-quality and accurate images of electricity poles, they differ in labor cost, time spent, and efficiency. In the subsequent sections, data collection methods will be elaborated in detail.

2.1.1 Conventional Methods

Inspecting power lines through conventional methods represents substantially manual and primitive approaches to image acquisition. Among these approaches, an experienced field team patrols the entire route corridor, preferably on foot or in an off-road vehicle (Aracil et al., 2002), or a climbing robot with an advanced camera attached to the power line and collects video/images (Katrašnik et al., 2010). During these processes, photos of utility poles can be gathered using binoculars and sometimes infrared and corona detection cameras (Katrašnik et al., 2010).

Although human visual observation demonstrates the capacity for accurate classification of tower anomalies over manual inspection methods, power lines extending across the extensive and naturally complex environment and visible surfaces of towers can only be observed from the ground. Consequently, the reliance on on-site personnel for data collection in comprehensive sites will likely result in high expenditures, diminished safety margins, and hazardous operational efficiency.

In response to the labor-intensive nature of conventional data acquisition techniques, the proposition of mobile robots (Figure 4) capable of traversing, ascending, and capturing video/images from electricity lines emerged as a prospective solution. These climbing robots are equipped with specialized cameras and are attached to power lines through the utilization of distinctive pins, enabling them to travel along the lines unceasingly. During the sliding process, cameras on the robots record many high-quality videos/images owing to the moving proximity to the electricity poles. Despite the evident advantages in efficiency, reduced labor intensiveness, and the acquisition of superior data, obstacles such as insulators, arresters, and cross-arms pose an intricate challenge (Katrašnik et al., 2010). In light of these complexities, semi-automated data collection methodologies grounded in aerial inspections became increasingly popular.



Figure 4. Climbing Robots over a Power Line

2.1.2 Semi-automated Methods:

The shortcomings of conventional image acquisition methods led to research into advanced techniques. These techniques are mainly based on collecting aerial images obtained by human-driven helicopters, satellites, and UAVs. The main advantage of using aerial tools for data gathering is collecting images more efficiently, accurately, and safely (Tong et al., 2010), unlike ground inspection and climbing robots.

One of the essential methods that provides automated data collection from very high distances is the application of remote sensing techniques. In other words, remote sensing mainly involves observing or collecting information about a target using a device positioned at a certain distance away (Cracknell, 2007). Given that this approach acquires data with high spatial resolution and facilitates the accumulation of extended data sequences distinguished by their consistent attributes (Xue & Su, 2017), it can be utilized to obtain optical satellite images. Nevertheless, it is imperative to acknowledge certain constraints associated with using satellite imagery.

Although utilizing very high-resolution images gathered by satellites is significant, it may not constitute an optimally efficient solution for the surveillance of power line corridors, considering factors related to weather conditions and matters of economic feasibility. Obtaining images, including the desired objects, is challenging when a cloud cover prevails in the desired area. Furthermore, obtaining and processing a high-resolution image is expected to be very costly (Matikainen et al., 2016). As a result, human-driven helicopters and UAVs are more reliable and suitable options for image acquisition from electricity poles.

Human-operated helicopters encompass a composite configuration, including a helicopter, a proficient camera operator, a camera apparatus, and a designated pilot. It is based on the collection of images by relying on the capabilities of the pilot and camera operator. In other words, high-resolution images of utility poles can be captured by experienced photographers or automated camera gimbals by utilizing

human-piloted helicopters (Business Bliss FZE, 2023). This approach facilitates the procurement of images with optimal clarity and permits efficient time allocation, even in arduous terrains.

Even while they are faster than manual approaches (Jones & Earp, 2001), helicopter patrols outfitted with specialized fixed cameras or a photographer have various drawbacks regarding their size and the stability of the camera view. Lack of maneuverability is one drawback of using helicopters for data collection. They occupy large spaces, severely limiting their capacity to move and hover, especially in crowded and complex environments. As a result, gathering images with desired viewpoints could be very challenging. Image degradation brought by the cameras' residual sightline motion is another potential issue that can arise while using helicopters (Prasad et al., 2016). In other words, images collected during patrols may need to be more precise or transparent due to camera shake.

As a result, UAVs are the best options for collecting high-quality, accurate, detailed images with feasible methods. The following parts will explain the detailed description and comparison of UAVs.

UAVs can be categorized into distinct types, namely fixed-wing, helicopter, and multicopters (Mohsan et al., 2023) (Figure 5). Each of these UAV categories presents its unique set of advantages and disadvantages; as a result, selecting the appropriate UAV type should be conducted on the nature of the issue and the prevailing environmental circumstances.



(a)





(b) (c)

Figure 5. Types of UAVs (a) Fixed-wing, (b) Rotary-wing (Helicopter), (c) Rotary-wing (Multi-copter) (Mohsan et al., 2023 & Stewart et al., 2021)

Fixed-wing UAVs exhibit a structural resemblance to conventional aircraft. Their configuration, including physical attributes and takeoff and landing procedures, indicates a critical familiarity. This UAV variant is characterized by its capacity to achieve significant flight velocities, consequently facilitating the comprehensive coverage of expansive regions. On the other hand, it has some issues related to launching and landing, whereas it could be a more cost-effective solution, especially for electricity line monitoring. Given that enhanced agility and lower flight velocity are favorable to heightened efficiency, helicopter or multi-copter UAVs are more advantageous for data collection purposes centered around electricity poles.

Table 1. Comparison of UAV types (Matikainen et al., 2016 & Mohsan et al., 2023 & Z. Li et al., 2011)

UAV Type	***Advantages***	***Disadvantages***
Fixed-wing	- Fast flying speed - Covering large areas	- Launching - landing problems - High Price
Rotary-wing (Helicopter)	- Hovering ability - Flying closer to the ground	- High price
Rotary-wing (Multicopter)	- Hovering ability - Low price	- Limited flight time

Helicopters and multicopters are known for their ability to hover and fly close to the ground (Matikainen et al., 2016 & Mohsan et al., 2023 & Z. Li et al., 2011). Since both vehicles can hover and easily launch-land, financial efficiency becomes the driving factor in selecting the best UAV for this study. The rotary-wing (helicopter) configuration is more expensive than its rotary-wing (multi-copter) counterpart. In contrast, the flight duration of multi-copters is constrained due to battery-related limitations. This study selects multi-copters as the main UAVs since they are less costly and more agile than other vehicles described above, as can be deduced from Table 1.

2.2 Data Processing Techniques

Data processing techniques primarily facilitate the extraction of significant structures, patterns, and information. These techniques are extensively employed to address practical challenges, particularly in computer vision (CV) and artificial intelligence (AI) applications. While the application domains of CV and AI are diverse, this study will use specific methods to address the challenges effectively.

Illustrative instances of these applications encompass the localization of target objects within images, the classification of images based on predetermined properties, and the identification of edges of images.

Throughout this study, the robust capabilities inherent to CV and AI applications will be harnessed to formulate a cohesive series of methodologies engineered to identify tilted electricity poles precisely. The proposed approach entails the integration of object detection models, a sequence of image processing techniques, and meticulous geometrical measurements to obtain a well-designed, highly accurate, and efficient solution. The literature study section will be divided into two sub-groups that includes:

- Research on the detection of electricity poles by deep-learning models
- Detection of tilted electricity poles by image processing and deep learning methods

2.2.1 Research on Detection of Electricity Pole by Deep Learning Methods

Object detection is a pioneering domain of inquiry that enhances the aptitude to address many real-world challenges. Within the framework of an object detection problem, annotated images are provided alongside their corresponding classes to a deep learning model, thereby enabling the derivation of an approximate spatial location of the target object as an output. This output commonly comprises four coordinates defining a rectangular bounding box encapsulating the object and assigning its class label. Several studies have researched the detection of electricity poles using object detection algorithms.

The initial paper (Zhang et al., 2018) focused on identifying a specific category of utility poles distinguished by the presence of cross arms, employing supervised learning techniques. The dataset for training the deep learning model was captured from the Google Street View application. These images were gathered through

screen capture methods facilitated by the application. Following the completion of the image-gathering process, a total number of 3500 screen views were annotated. This study selected the RetinaNet-101 architecture (Lin et al., 2017) as the preferred object detection algorithm. After the dataset preparation phase, the collection of input images was partitioned into distinct subsets, including training, validation, and testing categories.

During the training phase, 2,500 screen views were dedicated to training the model, while the residual 1000 images were evenly partitioned to validate and test the object detection algorithm. As part of the augmentation techniques, random horizontal flips were incorporated, employing a batch size of 1 and an epoch of 200. Upon culminating the training process, specifically for an intersection over union (IoU) threshold of 0.5, the model demonstrated an aggregate accuracy of 50%, precision reaching 73%, and a recall metric of 62%. Visual representations of the test results derived from the proposed model are exhibited in Figure 6.



Figure 6. Results of the Object Detection Algorithm (Lin et al., 2017)

In an alternate investigation, the utilization of two distinct object detection methodologies, namely Faster R-CNN (Ren et al., 2017) and YOLO-V3 (Redmon & Farhadi, 2018), were employed with the primary aim of detecting and classifying high-voltage transmission towers. This research examined four distinct typologies of power towers: drum-shape, umbrella-shape, wine-glass shape, and cathead-shaped

towers. The imagery employed in this study was acquired by deploying a specialized drone and ground-based cameras.

A range of augmentation techniques were employed to enhance the diversity and volume of the training dataset, including adjustments to brightness, rotation, and mirroring. Upon training two distinct deep learning models using identical input datasets, it was discerned that the Intersection over Union (IoU) values achieved by the Faster R-CNN model (0.882) exceeded those of the YOLO-V3 model (0.874). On the other hand, it is noteworthy that the YOLO-V3 model exhibited an average detection speed that was approximately 100 times faster when contrasted with the Faster R-CNN model.

In the work by (Nguyen et al., 2019b), a comprehensive methodology was outlined for the multi-stage detection of components and faults related to electricity poles. The proposed framework involves the application of Single Shot Multibox (SSM) detector (Liu et al., 2016) to detect components, while the identification and classification of minor parts and faults were executed through the employment of deep Residual Networks (He et al., 2016). The architectural design of the proposed model, as depicted in Figure 7, centers on the initial detection of utility poles. After this preliminary detection, the SSM detector is engaged and classifies the small-scale components associated with the power lines. In the concluding stage, the Residual Network classifies the identified and cropped components, discerning their specific fault classes.

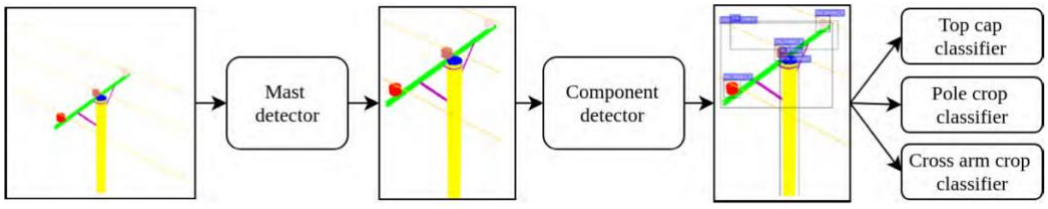

Figure 7. Steps of the Proposed Model (Nguyen et al., 2019b)

The dataset employed for training the model aimed at detecting components within power lines, including a total of 28,674 images with a size of 6048x4032. Some augmentation techniques, flipping, blurring, zooming, and rotation, were

implemented to augment the training dataset. Following the completion of the training process, the proposed model exhibited the capability to accurately identify utility poles, yielding an Average Precision (AP) of 88.00%. Moreover, the model demonstrated efficient classification proficiency for two distinct types of components, pole crops, and cross-arm crops, exhibiting weighted Precision values of 96.93% and 74.00%, respectively.

Sampedro et al. (2014) suggested an investigative approach, including two distinct stages: electricity tower detection and subsequent classification. This method uses Histograms of Oriented Gradient (HOG) features in conjunction with training two Multi-layer perceptrons (MLP). This research includes two sequential steps: (i) Detection of electricity poles and (ii) classification of the four distinct types of electricity towers. During the initial phase, a sliding-window technique systematically traverses the images. After each window's traversal, the corresponding window of the image delimited by the present window's boundaries is isolated, and its HOG features are extracted. These extracted features are subsequently employed as input vectors to a first-layer MLP classifier to determine whether the given window section constitutes a component of an electricity tower or belongs to the background (Figure 8).

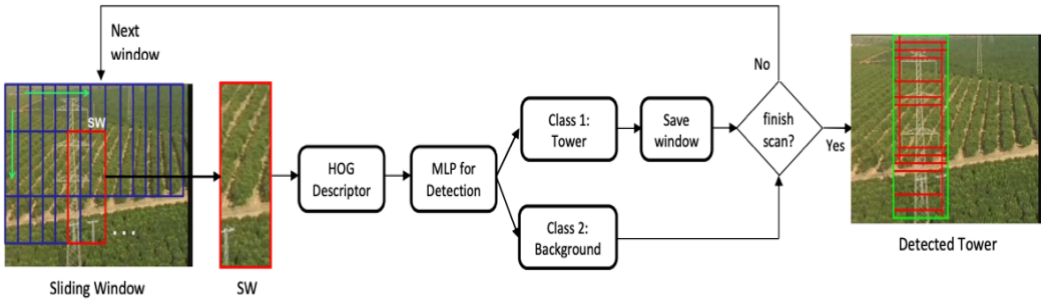

Figure 8. Detection of Electricity Tower

Upon the culmination of the window scanning procedure, the ultimate bounding box, including the electricity towers, was gathered by aggregating foreground window sections. In the subsequent stage, the outcomes derived from the initial stage –

specifically, the coordinates of the bounding boxes – were employed to crop the objects. Analogous to the initial step, the HOG features of these cropped objects were extracted. This dataset was then used to train a Multi-layer perceptron (MLP) classifier with four distinct classes, facilitating the classification of towers based on their respective types (Figure 9).

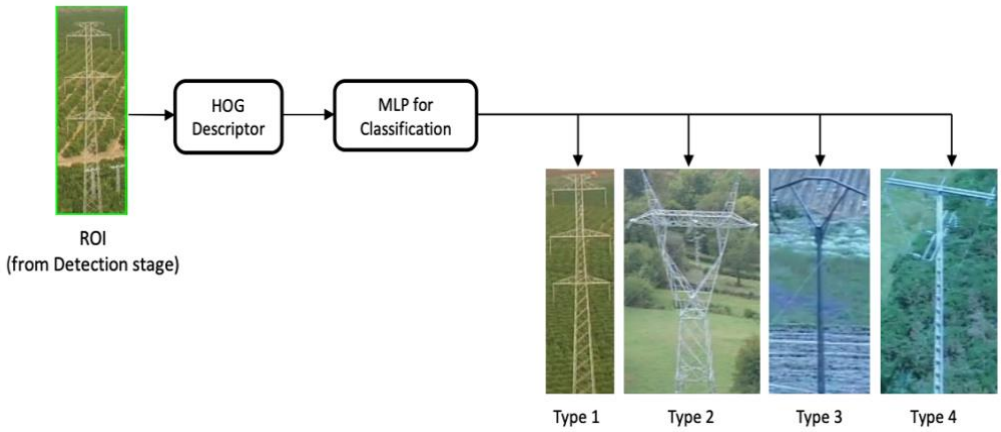

Figure 9. Classification of Towers

For dataset generation, a collection of 11 aerial videos was captured utilizing Unmanned Aerial Vehicles (UAVs), enabling the cropping of electricity towers from these recorded sequences. Consequently, a dataset comprising 3200 images was created, with an equal distribution of 1600 images for tower sections and the same number of images representing background sections. The evaluation of the first stage of the methodology provided accuracy values of 91.67% and 75% for the classification of tower and background segments, respectively. Subsequently, the classification of towers based on their types exhibited accuracy values of 93.33%, 86.67%, 60%, and 86.67% for the respective four classes.

2.2.2 Detection of Tilted Electricity Poles by Image Processing and/or Deep Learning Methods

Numerous scholarly investigations have been dedicated to detecting and classifying electricity poles, employing the capabilities of image-processing techniques and

deep-learning methodologies. In a specific instance, the work presented in (Varghese et al., 2017) introduced a sequence of successive deep learning approaches that aim to detect the electricity poles and their tilt degree based on images acquired through UAVs. In the initial phase of this research (Figure 10), a pre-trained deep learning model was employed as a foundational feature extractor. After this, a set of specialized layers was introduced to the model's architecture for detecting electricity poles.

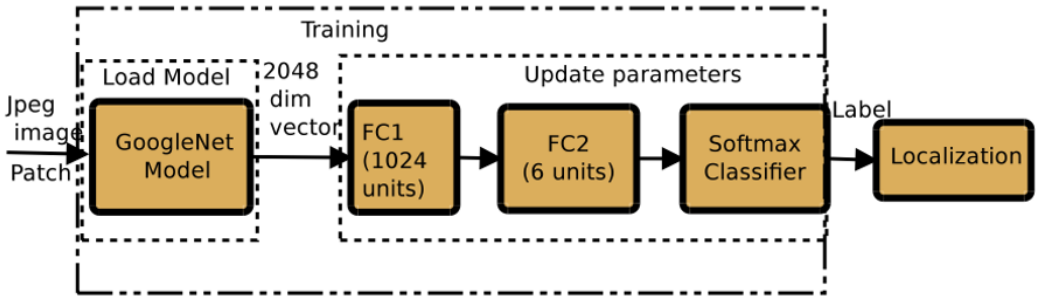

Figure 10. Architecture of the Proposed Method (Varghese et al., 2017)

Once the precise localization of poles within the images was established, a post-processing algorithm based on a graph-based approach was applied. This algorithm serves the purpose of eliminating any false positive bounding boxes that include undesired elements. Thus, the output produced by the deep neural network was employed as the input for this post-processing algorithm, facilitating the accurate removal of erroneously detected bounding boxes. Electricity poles' tilt angles were measured in the investigation's subsequent phase through a comparative analysis involving two sets of images: test images, which may exhibit varying degrees of tilt, and reference images, including perfectly upright electricity poles. The methodology utilized geometric principles by fitting ellipses to test and reference pole images. The deviation in the orientations of the major axes of these fitted ellipses provided the measure of tilt degree. The efficiency of the proposed approach was validated, and a dataset containing 150 images was employed for testing purposes. The evaluation metrics values are 87.79% (F-Score), 97.90% (Accuracy), 93.50% (Precision), and 83.6% (Recall).

Chen and Miao (2019) suggested a methodology for detecting electricity poles by determining their numerical count and risk status. This method utilized images and videos captured by UAVs, and the proposed approach was organized as follows: (i) Detection of electricity poles and (ii) Classification of the electricity poles concerning their orientation, upright or fallen. During the initial stage, images were extracted from the recorded videos captured by UAVs. Since the number of videos, including fallen poles, was insufficient, a strategy was implemented to simulate such instances by introducing a complex background (Figure 11).



(a) (b)

Figure 11. Simulated images representing (a) Upright pole, (b) Fallen pole (Chen & Miao, 2019)

In the training phase for the detection of poles, a comprehensive dataset containing 13,429 images was utilized. Within this dataset, 11,951 images were dedicated to the training set. The YOLOv3 (Redmon & Farhadi, 2018) architecture was the chosen framework for the training procedure. In this context, the model was augmented with a Region of Interest (ROI), which served the model with indications regarding the approximate locations of electricity poles within the images. This assessment was achieved by estimating the positions of objects situated centrally within the images (Figure 12).

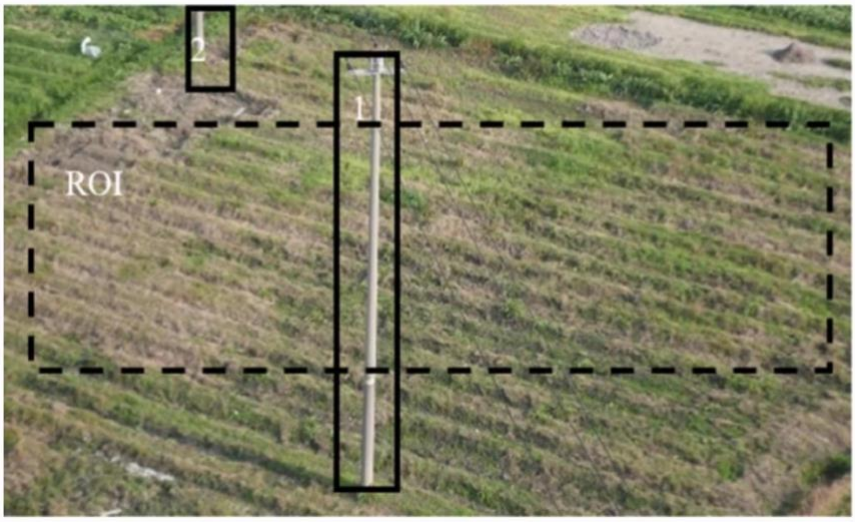

Figure 12. ROI in the Middle of an Image (Chen & Miao, 2019)

After enhancing and training the YOLOv3 model for the dual tasks of pole detection and classification, the achieved performance was reflected in the Average Precision (AP) metrics. Specifically, an Average Precision value of 90.09% was obtained for upright poles, while fallen poles exhibit an Average Precision value of 90.81%.

Hosseini et al. (2020b) enhanced a comprehensive methodology to detect potential damages that could occur on electricity poles. This approach was developed through the integration of four distinct models: (i) Damage classifier, (ii) Destruction estimator, (iii) Pole detector, and (iv) Fire detector (Figure 13).

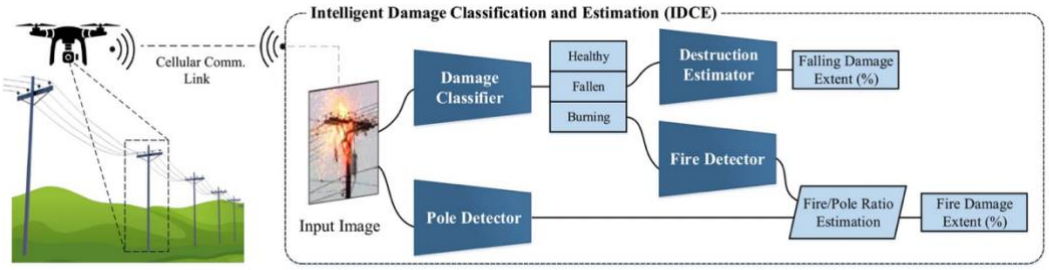

Figure 13. Representative architecture for the proposed model

Within the framework of the damage classifier model, a Convolutional Neural Network (CNN) was trained to classify images into three distinct classes: healthy, fallen, and burning poles. After the classification process, fallen poles were grouped,

facilitating the subsequent application of the destruction estimator model. This latter model served the purpose of providing a scalar value that quantifies the extent of damage. This quantification was achieved by introducing a 14x14 pooling layer at the final stage of the model's architecture (Figure 14).

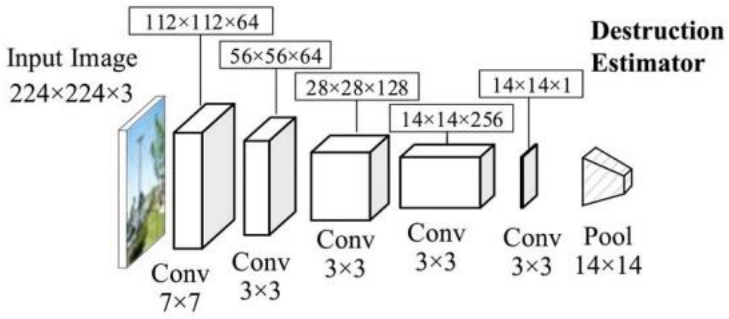

Figure 14. Architecture of the Destruction Estimator Model

The pole detector model was applied to the bounding box, including electricity poles, in the fire detector model context. The ratio of pixels associated with fire to the total pole area was computed by assessing the fire extent. For the entire model, a dataset comprising a total of 1615 images was employed. This dataset encompassed 572 images of healthy poles, 457 of fallen poles, and 586 of burning poles. Three distinct augmentation techniques were implemented to augment the dataset and diversified its contents, including Five-crop, random horizontal flipping, and color jittering. During the training procedure, the images were partitioned into distinct datasets utilizing ratios of 0.6 for training, 0.2 for validation, and 0.2 for testing, respectively. The accuracy value for the damage classifier model was 94.54%, and the error rate of the destruction estimator was 15.43%. In contrast, the estimation error for the pole and fire detector models was 21.56 pixels.

The investigation conducted by L. Li et al. (2021) centered on the determination of tilt angles of the electricity poles with a distinctive emphasis on the utilization of satellite optical imagery. Within the framework of satellite images, the detection of tower shadows by electricity poles was comparatively more straightforward than the direct detection of the poles themselves. Consequently, the preliminary phase of this

research focused on the extraction of tower shadows with an implementation of the K-means clustering algorithm (Lloyd, 1982). In shadow detection, the contours of the identified shadows were subjected to applying the Hough line detection algorithm (Figure 15).

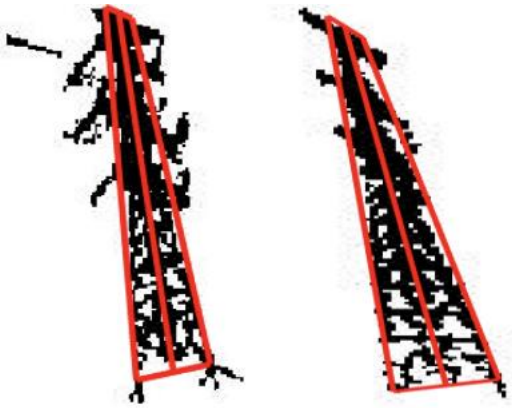

Figure 15. Representation of the Shadows and Geometric Centerlines of Towers (L. Li et al., 2021)

Additionally, other parameters, including solar altitude and azimuth angles, were computed based on the precise moment of image acquisition. Proceeding to the third phase of the methodology, essential input data, including the actual tilt degree of the towers, the length, and orientation of the detected contour centerline, as well as the solar altitude and azimuth angles, were collectively provided to a three-layer Back Propagation (BP) Neural Network. This neural network estimated the tilt angle of the electricity poles. In training, 80 shadow images corresponding to the towers are utilized, while the test set contains 26 such images. The proposed model reached an accuracy rate of 92.31%.

2.3 Gaps in the Literature

The comprehensive review of existing literature about the detection of tilted electricity poles has yielded valuable insights into various approaches and recommendations to enhance the reliability and robustness of models. Nonetheless,

the investigation has brought to light several notable deficiencies, which serve as the focal points of this study's inquiry. These primary gaps encompass the following:

- Limited utilization of real electricity pole images in research endeavors,
- Inadequate utilization of structured methodologies for image acquisition,
- Absence of rigorous geometric principles in the determination of electricity pole tilt angles and
- There is a need for more validation of the detected representative lines for electricity poles.

The initial gap pertains to the need for actual images. Given the need for comprehensive electricity pole image datasets within the existing literature, specific simulated electricity pole images were generated for comparative purposes. While these images may serve as training data for deep learning models, it is imperative to note that the outcomes derived from such models may lack reliability and may not accurately capture real-world scenarios.

Another noteworthy gap is the need for a meticulously designed image acquisition guide. Such a guide would ideally furnish precise directives for capturing electricity pole images, including specified distances and elevations. Consequently, this standardized approach would yield a uniform perspective in images sourced from various electricity poles, thereby enhancing the robustness and reliability of training methodologies for deep learning models.

Assessing an electricity pole's inclination angle represents a pivotal phase within a risk detection model. Within the extant literature, the application of geometric principles to quantify the tilt angle of electricity poles are notably absent despite the inherent accuracy and reliability associated with such an approach. This matter is also intricately linked to the inadequacy of images collected directly aligned with the poles. This factor substantially enhances the precision of tilt angle calculations when employing images as input.

Finally, it is worth noting that certain studies have adopted the practice of extracting contours from electricity poles for tilt angle measurements. While this approach holds merit, it is imperative to underscore that the detected lines are not subjected to validation procedures to verify their faithful representation of the correct shape of electricity poles.

These deficiencies identified in the existing literature provide the foundation for developing an encompassing model. This model leverages real imagery of electricity poles acquired through UAVs, uses the computational prowess inherent in deep learning and image processing methods, employs fundamental geometric principles for precise tilt angle measurements of the electricity poles, and rigorously enhances the validation of the detected representative lines for the electricity poles. The subsequent chapter will delve into a detailed examination of the proposed method.

CHAPTER 3

METHOD OF TILTED ELECTRICITY POLES DETECTION

This chapter comprehensively explains the method employed to detect insecurely tilted electricity poles. The primary objective of this method is to minimize manual interventions within electricity grid operations, paving the way for the development of an autonomous and exact suite of artificial intelligence models. This chapter will delve into the fundamental principles underpinning the detection model while offering an intricate elucidation of the algorithmic architecture.

The proposed method consists of four main steps: (1) object detection method, (2) advanced image processing techniques, (3) validation of the detected lines and (4) risk classification method. As an initial step, the detection of approximate locations of electricity poles within the provided images is accomplished by deploying an object detection method, the Faster R-CNN (Ren et al., 2015). This model aims to detect bounding boxes encapsulating the electricity pole structures. After this stage, the coordinates derived from the detected bounding boxes are employed to effectively filter out the environmental artifacts surrounding the poles, including elements like trees, road markings, and buildings. Besides detecting bounding boxes, the proposed object detection model undertakes the classification of the electricity poles based on their respective structural materials, according to their categories, such as concrete, steel, or wooden poles.

The subsequent phase within this model uses the output values of the object detector. These outcomes are as the cropped portions of the images, containing exclusively the electricity poles. Subsequently, an array of image-processing techniques is employed to estimate a line that effectively represents the inherent structures of the poles. In the subsequent stage, a comprehensive evaluation of the detected

representative pole lines is conducted by some performance metrics to comprehend the robustness and effectiveness of the proposed method.

In the last phase, two consecutive components, (a) Measurement of the tilt angles and (b) Classification of the risk status of the poles based on these angles utilizing pre-established angle thresholds, are applied. The initial component deals with the determination of the inclination angle of the electricity poles. This quantification is achieved by utilizing algorithms that inherit the established geometric principles.

Following the prevailing design patterns, certain pole types may exhibit variable configurations. For instance, steel poles might inherently possess natural structural inclinations, whereas this property is not valid for concrete/wooden poles (Figure 16). Consequently, different threshold values become necessary for the various types of poles.

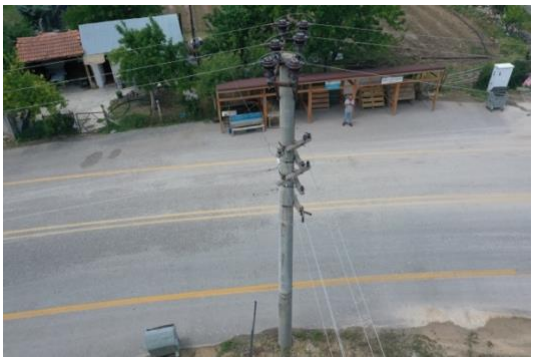

(a)



(b)



(c)

Figure 16. Comparison of Natural Inclination of Pole Types (a) Concrete Pole without Natural Structural Inclination (b) Wooden Pole without Natural Structural Inclination (c) Steel Pole with Natural Structural Inclination

In the last part of the third step, the determination of the risk status of the poles is established based on their respective tilt angles. This process is conducted by deploying an algorithm designed to examine whether the prevailing inclination angle of the electricity poles surpasses the pre-determined threshold limit. A flowchart of the process for detecting tilted electricity poles is visually depicted in Figure 17, while the details of each step will be comprehensively explained in the forthcoming sections.

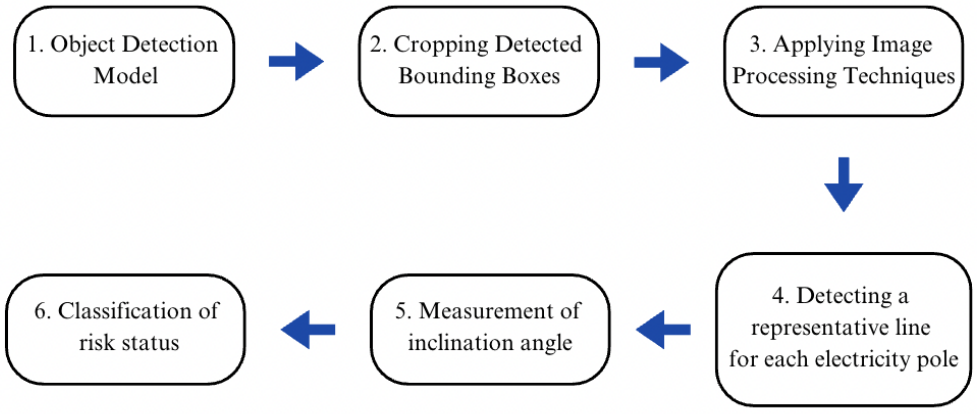

Figure 17. Flowchart of the Proposed Risk Classification Method

3.1 Object Detection Algorithms:

The initial phase within the risk detection model for tilted electricity poles includes identifying electricity poles through input images with dimensions of 5472x3648. During this stage, the procedure of image labeling is imperative to create distinct training and testing datasets for the model. This image labeling process necessitates the meticulous drawing of bounding boxes around the electricity poles, a task that is performed manually. To facilitate this particular step, labeling software has been employed.

Following the completion of the labeling procedure, the images and their labels, bounding box coordinates, and the classes of the pole types are split into train-test sets, maintaining a split ratio. The object detector model learns from the training

dataset, subjecting its learned capabilities to evaluating previously unseen data within the test set. During the training phase, several critical considerations concerning the deep learning models require careful attention. These considerations encompass the image labeling procedure and selecting an appropriate object detector type and its properties. Comprehensive details of each step of the model will be discussed in the forthcoming sections.

3.1.1 Image Labeling Procedure

Image labeling is one of the significant steps of deep learning models. This procedure aims to create bounding boxes with rectangular shapes that enclose the boundaries of the target objects. These bounding boxes are created with four corner coordinates of a rectangle. The main challenge of this procedure is drawing the best tight rectangle that includes all the parts of the objects while the environmental noises should be excluded as much as possible.

An indispensable point of the labeling procedure is the precise allocation of object classes. Within the framework of this study, the objects are classified into three distinct classes that correspond to different types of electricity poles: concrete, steel, and wooden (Figure 18). Upon the detection of the bounding box coordinates, the electricity pole classes are assigned based on the underlying material composition of the respective poles.



Figure 18. Concrete, Steel, and Wooden Electricity Pole Images

During this study, a total number of 8775 images that contain electricity pole instances were annotated by an approximate effort of 175 person*hours. An original in-home software has been utilized to create and store the annotations. Each image, accompanied by its associated coordinates and class labels, is meticulously stored within a database within this software framework. Furthermore, the software can generate a comprehensive summary of labeled images in a JSON file.

3.1.2 Object Detector

An object detector's foremost objective is identifying the approximate spatial locations of the target objects within the given images. The detector accepts a batch of labeled images as input. Subsequently, the object detector proceeds to learn from the provided information, encompassing the coordinates of bounding boxes and the designated classes of the objects. In alignment with the objectives of this study, an object detector has been devised that leverages both supervised learning and transfer learning methodologies.

Supervised learning (B. Liu, 2011) represents a specific machine learning method, characterized by its reliance on labeled datasets to facilitate the training of models. The output of such models is classifying test images or estimating the spatial coordinates of detected objects in the context of object detection. This learning mode can be analogous to Kolb's learning cycle (Kolb, 2014), wherein the human learning process is likened to a cyclical progression. According to this theoretical framework, the human mind learns knowledge from past experiences and actions. Consequently, when confronted with inexperienced situations, the mind utilizes prior experiences to respond.

Supervised learning has been notably influenced by this inherent learning phenomenon, i.e., exploration of knowledge acquisition from labeled datasets. Analogously, the past experiences of a human being find representation in the form of labeled datasets. At the same time, novel scenarios correspond to the unseen datasets encountered within the domain of deep learning models.

Another crucial step in the training of a deep learning model is the determination of weight values. Throughout model training, these weight values are initialized, assuming a pivotal role in the efficiency of the learning process. As a result, the initial values attributed to a model's weights pose substantial significance. In this study, the process of selecting initial weight values has been undertaken using transfer learning methodologies.

In the transfer learning technique, the final weights of a previously trained model have been utilized as the initial weight values of a current deep learning model. In other words, the weights of another pre-trained model have been transferred to a model that will be trained. This method enhances the performance and rapidness of a current deep-learning model by decreasing the expected training duration (Goodfellow et al., 2016) (Figure 19).

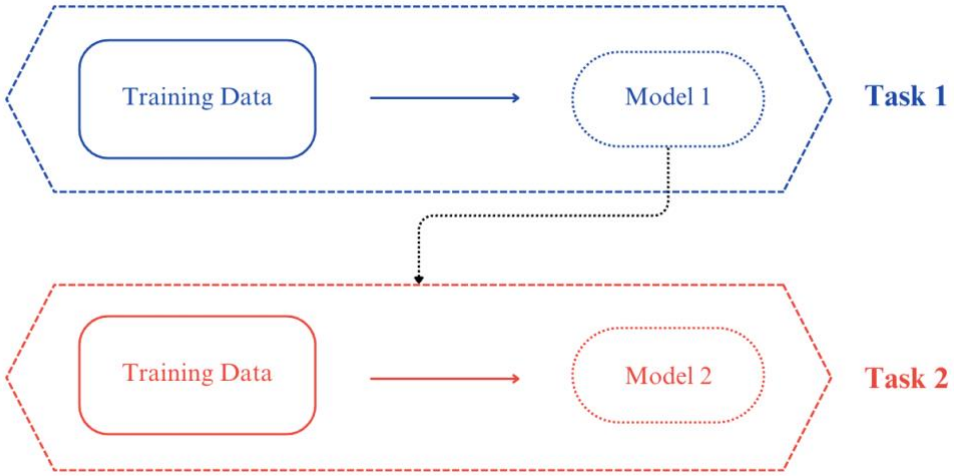

Figure 19. Representation of Transfer Learning Method

This study has executed the process of detecting bounding boxes by employing a widely recognized and extensively employed object detection framework, Faster R-CNN (Ren et al., 2015). This methodology has been utilized with supervised learning mechanisms supported by integrating transfer learning techniques. Faster R-CNN stands as a distinguished object detector that consists of sequential sub-models to manage high-resolution RGB images efficiently. The fundamental architecture of the Faster R-CNN model encompasses an array of convolutional layers, complemented by a Region Proposal Network and a Region of Interest Pooling (RoI) layer (H. Wang et al., 2019). The detailed functions of these layers will be explained in the following sections by utilizing Figure 20:

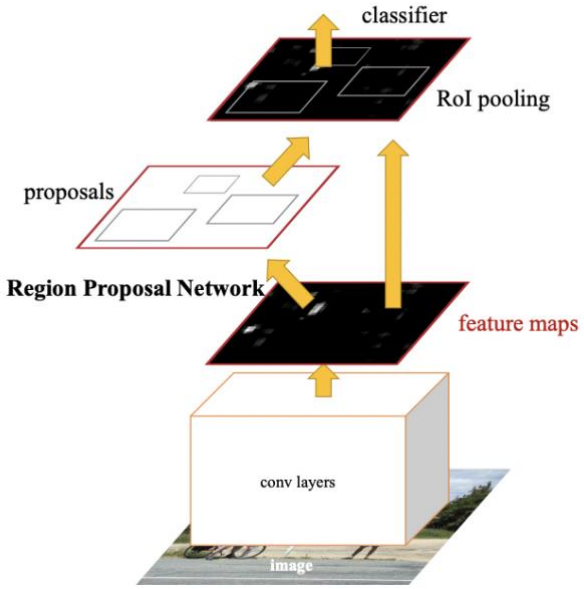

Figure 20. Representative Architecture of Faster R-CNN (Ren et al., 2015)

- **A Set of Convolutional Layers:** At this step, convolution layers with the ReLU activation function and pooling layers are applied to extract the features of the provided images.
- **Region Proposal Networks (RPN) Layer:** This framework is used to generate region proposals that encapsulate the targeted objects. Employing Softmax functions, these layers discern whether the proposed anchors or region proposals belong to the foreground or the background. At the final stage of this step, a bounding box regression technique is deployed to rectify the anchors to attain precise object localization.
- **Region of Interest Pooling Layer:** This model component aims explicitly to collect the feature map with the region proposals and synthesize these distinct information sources. Proposal feature maps are produced after the information extraction process, serving as the foundation for subsequent layer operations. These subsequent layers encompass a fully connected layer that determines the classes to which objects belong and a classification layer that computes the definitive and meticulous positioning of the bounding boxes.

Several pivotal properties were incorporated throughout the Faster R-CNN object detector training phase. These inherent properties encompass the selection of the classification and feature extractor models. Within object detection, a deep learning model, ResNet-50 (He et al., 2016b), were employed to classify the diverse electricity pole types. Simultaneously, the feature extraction process is facilitated by incorporating Feature Pyramid Networks (FPN). The details of these two models will be examined in the following sections.

3.1.2.1. Resnet-50

A deep learning model includes multilayered artificial neural networks. These models often comprise numerous layers, thereby facilitating the attainment of high accuracy and efficiency. Throughout the training phase of the model, these neural layers undergo iterative updates conducted by backpropagation algorithms. These algorithms employ optimization techniques to calculate the error functions, ultimately guiding the model towards improved performance (Tan & Lim, 2019). The representation of a block of a deep neural network is indicated in Figure 21.

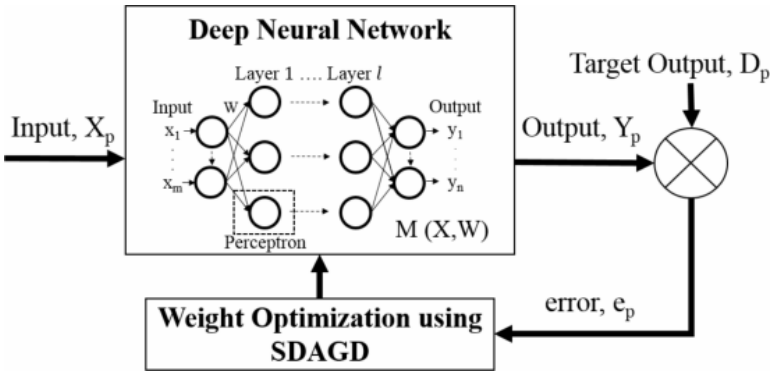

Figure 21. A representation of a deep neural network (Tan & Lim, 2019)

Upon completing the initial forward pass during the training phase, an output is generated following the nature of the problem under consideration. For instance, a class probability or class label would be the output of a classification model. This resulting output is subsequently combined with the target output, thereby facilitating

the assessment of the model's capacity to approximate the target outcome. The neural network's weights are updated according to the error function derived from the difference between the obtained and intended output values. This procedure is recognized as backpropagation. This iterative adjustment of weights is executed to enhance the model's predictive performance. The backpropagation process has been conducted by calculating the gradients, which the following equation can represent:

$$\frac{\partial L}{\partial W} = \left[\frac{\partial L}{\partial w_1}, \frac{\partial L}{\partial w_2}, \frac{\partial L}{\partial w_3}, \frac{\partial L}{\partial w_4} \dots\right] \quad (1)$$

Where L represents the error function, while W is the vector of neural network weights, throughout the training phase of a model, a sequence of forward and subsequent backward passes is a recurring phenomenon, culminating in the calculation of multiple derivatives of the error function in relation to the weights. While the increase in the neural network's layer count is expected to mitigate the error rate of a model, it is imperative to acknowledge that the adoption of deeper architectures might cause the Vanishing/Exploding gradient problem. This issue were studied, and it is demonstrated that an increase in the number of layers is the main reason for gradients' being close to 0 or very large (Kaiming et al., 2015).

This phenomenon is tested with two Convolutional Neural Networks (CNNs) (O'Shea & Nash, 2015) that have 20 and 56 layers, respectively (Figure 22).

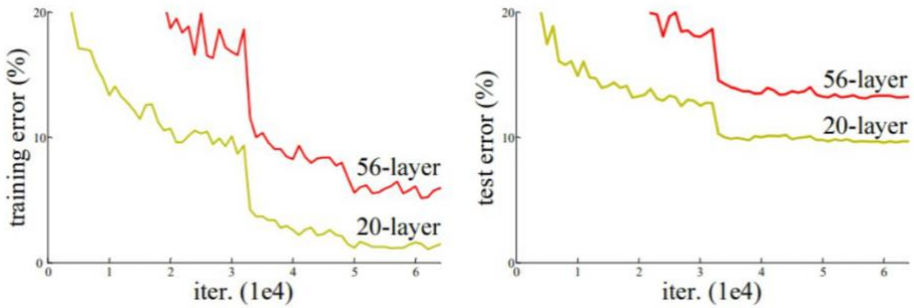

Figure 22. Comparison of Two Neural Networks with Different Number of Layers (He et al., 2016b)

From these plots, it can be observed that 56-layer CNN has a higher error rate for both training and testing processes than 20-layer CNN. This deduction emphasizes the significance of addressing the Vanishing/Exploding gradient issue. To mitigate this phenomenon, one prominent way of investigation is Residual Networks (ResNet) (He et al., 2016b).

ResNet is one of the significant deep learning models with a well-known and inspiring method of Residual Blocks (Figure 23) against the Vanishing/Exploding gradient problem (Hochreiter, 1998). In Residual Blocks, a technique called skip connections has been utilized, which mainly aims to connect the activation of weights of a layer to the further layers. In other words, activation of weights is added to the additional layers by skipping some layers in between.

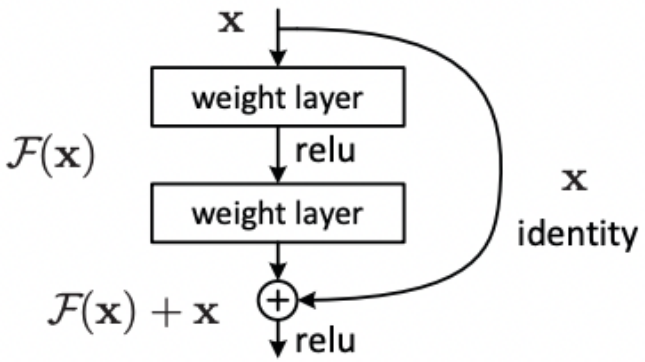

Figure 23. Representation of a Residual Block in ResNet (He et al., 2016b)

Skip connections enable Residual Blocks to form, and the stacking of these blocks results in Residual Networks. The mathematical representation of this model can be seen in the following equation:

$$H(x) := F(x) + x \tag{2}$$

Where x represents the weight vector of the current layers, $F(x)$ is the output of the forward layer, in which the activation function is applied. Adding previous layers' weight values with the current layers' activated output prevents the occurrence of

Vanishing/Exploding gradients. This pivotal architectural framework facilitates the construction of deep learning models characterized by an extensive depth of layers.

3.1.2.2. Feature Pyramid Networks

Artificial Neural Networks (ANN) (Jain et al., 1996) mainly consist of artificial neurons that aim to imitate human natural neurons. An ANN primarily consists of an input layer, some hidden layers, and an output layer (Figure 24).

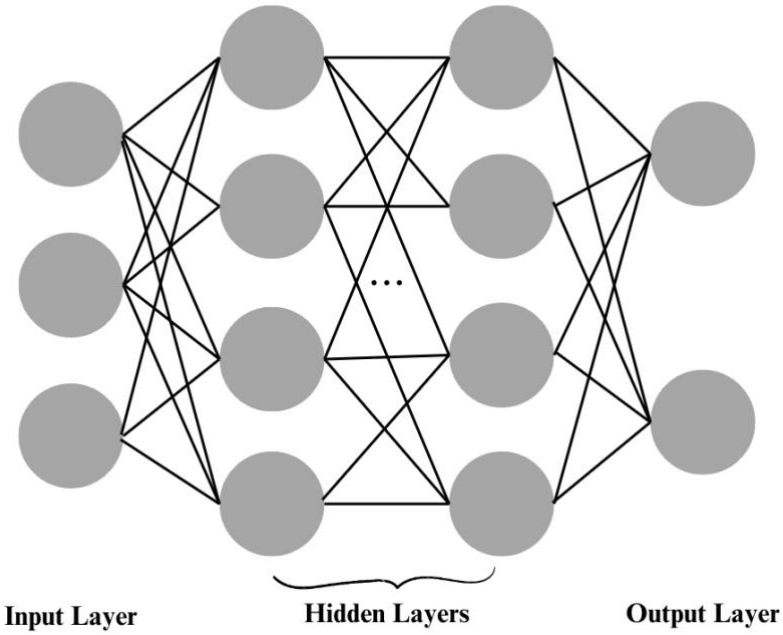

Figure 24. Representative Artificial Neural Network (ANN)

In the input layer, the pixel values of each image serve as input values. These input values are subjected to multiplication by pre-established weights and subsequently added with a constant value unique to each artificial neuron. This fundamental equation represents a linear calculation. The following equation indicates the representative linear calculation of a neuron:

$$z = W * x + b \quad (3)$$

In this context, the symbols W, x, b, and z denote a weight vector, an input vector, a bias constant, and an output vector, respectively. This calculation is systematically executed across all neurons within all layers within linear models. Nonetheless, the performance metrics of linear models, such as sensitivity, specificity, and accuracy, tend to yield results of lesser efficacy than non-linear models (Landi et al., 2010). In establishing a non-linear model, applying an activation function is essential. The representative non-linear equation of a neuron can be seen in the following equation:

$$z = \sigma(W * x + b) \quad (4)$$

where σ represents an activation function. The initial layer receives the input data from the external sources, subsequently forwarding this data to the hidden layers. In this layer, every neuron utilizes the outputs derived from the preceding layers, with the resultant values serving as inputs to the output layer. Across these successive passes, the provided data undergoes a comprehensive analysis with simultaneous training and learning processes. In other words, as the input data transfers through consecutive layers, the artificial neural network progressively learns deeper insights from the attributes of the provided dataset.

CNNs are one of the types of ANN containing particular layers: convolutional and pooling layers and fully-connected ones (O'Shea & Nash, 2015). In the next section, the details of each layer will be explained.

a) Convolutional Layer

A convolutional layer is the first processing step of an input image. During this step, learnable kernels, specialized small-sized matrices, convolve each part of the provided images (O'Shea & Nash, 2015). The convolution means synthesizing the given images by applying many elementwise multiplications of portions of an image and the kernels. The representative figure of the convolution can be seen in the following figure.

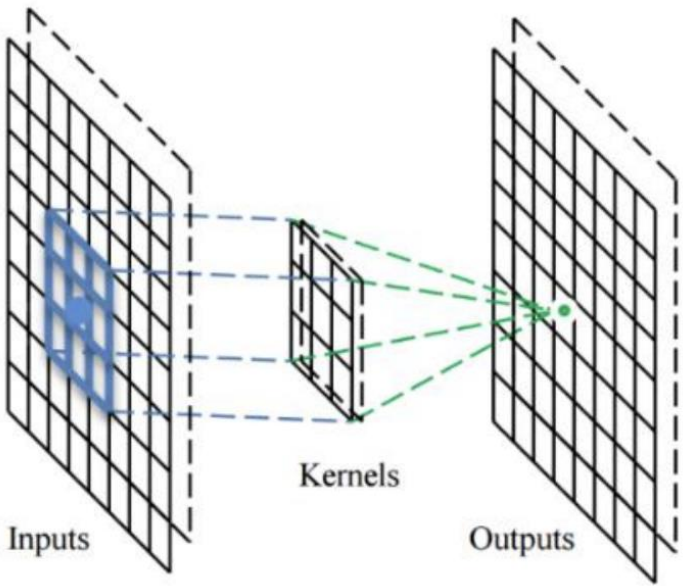

Figure 25. Representation of a Convolution Process (Zhang et al., 2018b)

As it can be deduced from Figure 24, the 3x3 portion of the provided image, inputs, are convoluted by the 3x3 kernels. At the end of a convolution process, the summation arising from the element-wise multiplication of the constituent elements of two distinct 3x3 matrices is acquired.

b) Pooling Layer

The core objective of the pooling layer is the reduction of matrix dimensionality, thereby decreasing the total count of model parameters. Within this layer, the convolved images serve as the input, and pooling is executed by applying precisely sized kernels. An illustration of the pooling process employing a 2x2 kernel is depicted in the following figure:

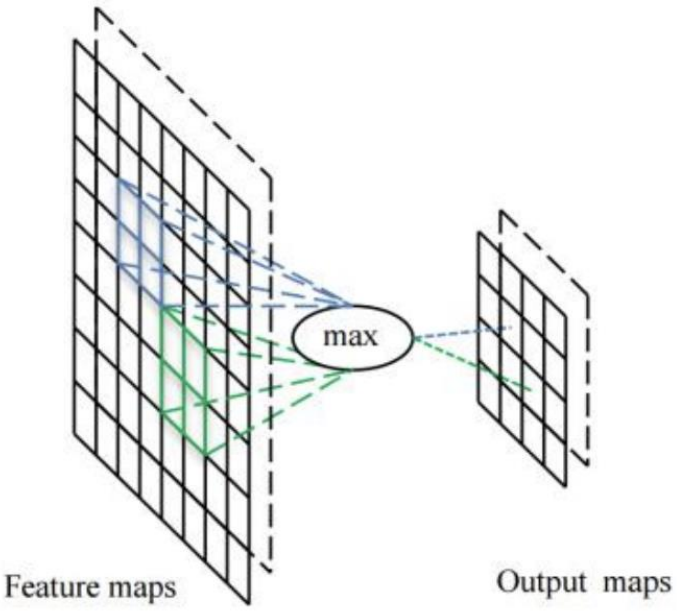

Figure 26. Representation of a Pooling Process (Zhang et al., 2018b)

In Figure 25, the maximum values of the 2-by-2 matrices of the feature maps are extracted from the output maps. Thus, the size of the feature maps is halved by selecting the higher pixel values.

c) Fully-connected Layer

The final layer of a Convolutional Neural Network (CNN) comprises interconnected neurons arranged in a configuration reminiscent of the conventional architecture of an Artificial Neural Network (ANN), as depicted in Figure 23.

Convolutional Neural Networks (CNNs) represent a pivotal class of deep learning models proficient in feature extraction from the provided input images. In the context of Feature Pyramid Networks (FPNs) (Lin, Dollár, et al., 2017), this architectural configuration facilitates extracting semantically robust features, like CNNs. However, FPN's outputs are merged with the previous layers' feature vectors (Figure 27).

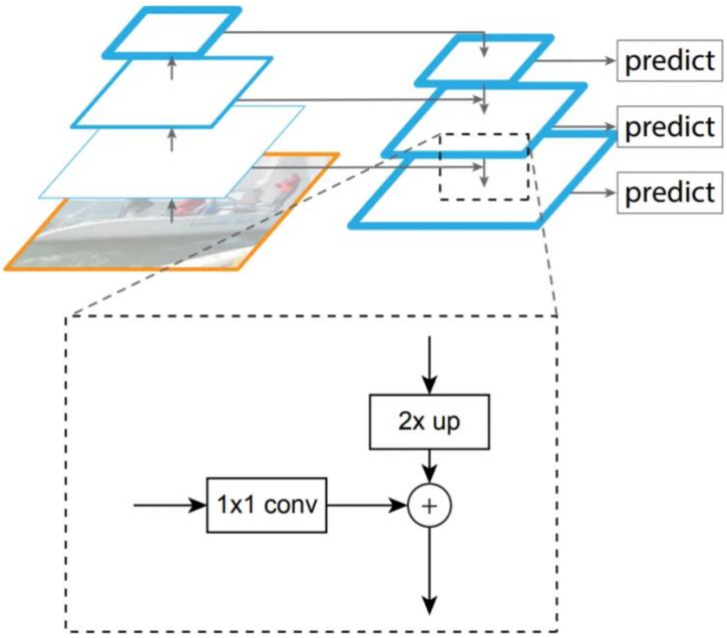

Figure 27. Feature Pyramid Network Architecture (Lin, Dollár, et al., 2017)

As can be seen from the figure, Feature Pyramid Networks (FPNs) are characterized by two distinct pathways: the Bottom-Up and the Top-Down paths. In the Bottom-Up path, a standard CNN is employed to derive a feature vector at the top of the initial pyramid (as illustrated by the left-side architecture in Figure 26. However, the Top-Down path utilizes the process of feature vector upsampling. This is achieved by integrating feature vectors from the Bottom-Up layer with the lateral connections (Lin, Dollár et al., 2017). Thus, the FPN structure provides semantically stronger features for the deep learning models, and they are utilized for the Regional Proposal Networks (RPN) in the Faster R-CNN model.

Following the production of bounding boxes by the object detector, which effectively encapsulates electricity poles, a series of consecutive image processing techniques are employed to discern a representative line that accurately identifies the poles. In the following section, details of these methods will be discussed.

3.2 Advanced Image Processing Techniques

The subsequent phase of the proposed methodology involves the application of a sequence of advanced image processing techniques to estimate representative lines for the electricity poles within the images. Within this step, the output values obtained from the preceding model, which encompass the coordinates of bounding boxes of electricity poles, are employed as input. The main reason for incorporating an object detection model before this second phase lies in its capacity to mitigate the potential interference sources that could adversely affect the effectiveness and precision of the method.

Electric pole images are cropped according to the bounding box coordinates (Figure 28).

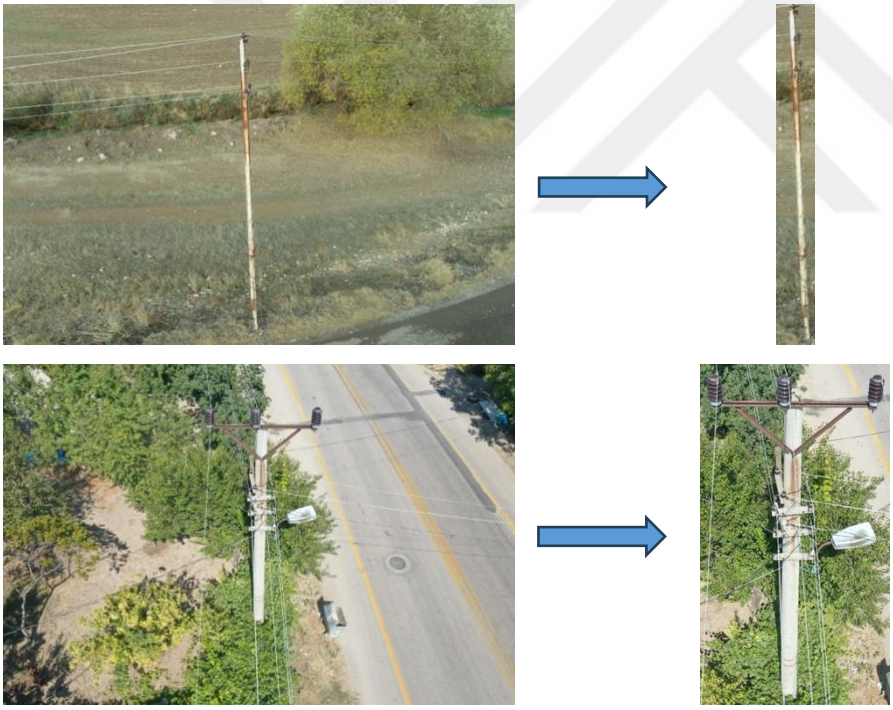

Input Images *Cropped Images*

Figure 28. Cropping of the Bounding Box Coordination

Within the preparation of the input images are completed, the following image processing techniques are applied consequently:

1. Converting RGB image to grayscale image
2. Applying gaussian blur
3. Applying morphological operations
4. Utilizing Canny Edge Detection model
5. Applying Line Segment Detector
6. Filtering the detected lines according to its length
7. Extracting the edges by thresholding
8. Applying Hough Line Transform
9. Finding the best line that represents the electricity poles
10. Measurement of tilt angles of the poles

In the following sections, the abovementioned image processing techniques will be explained by providing sample input images.

3.2.1 Converting RGB image to Grayscale image

In the first step of image processing techniques, RGB images are converted into Grayscale ones. An original image has three channels: Red, Green, and Blue (Figure 29).

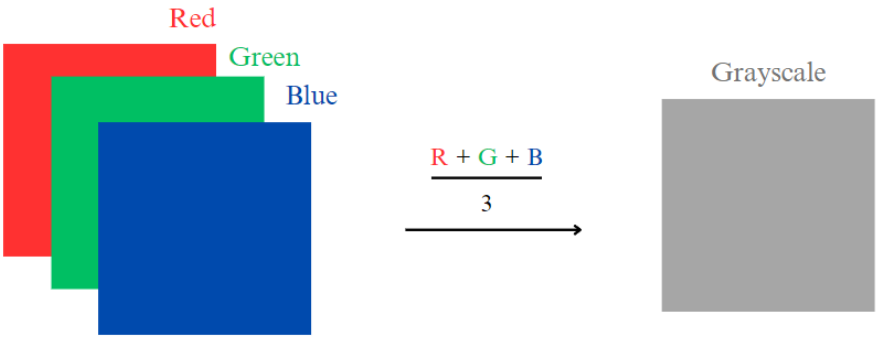

Figure 29. Representation from RGB Image to Grayscale Image

The conversion of an RGB image to grayscale requires the computation of the average value across the three-channel matrices. In other words, pixel values of all

the matrices are summed, which is subsequently divided by 3. The sample calculation can be seen in the following representation:

$$\left(\begin{bmatrix} r1 & r2 \\ r3 & r4 \end{bmatrix} + \begin{bmatrix} g1 & g2 \\ g3 & g4 \end{bmatrix} + \begin{bmatrix} b1 & b2 \\ b3 & b4 \end{bmatrix}\right)/3 \quad (5)$$

In this step, input data are the cropped images that are obtained by the result of the object detector, and the output is the image in grayscale.

3.2.2 Applying Gaussian Blur

During this phase, grayscale images serve as the input data, and Gaussian blur is applied to blur the provided image. The Gaussian blur algorithm utilizes the convolution process with a kernel, the coefficients of which are determined by using the Gaussian Normal Distribution function (6) (Gedraite & Hadad, 2011).

$$G(x,y) = \frac{1}{2\pi\sigma^2} e^{-\frac{x^2+y^2}{2\sigma^2}} \quad (6)$$

Upon the computation of convolution matrix values using the Gaussian function, the input image is convolved with this kernel, generating an output-blurred image. The mathematical representation of an output of blurred images can be seen in the following equation:

$$Y(i,j) = \sum_{u=-w}^{w} \sum_{v=-w}^{w} X(i+u, j+v) G(u,v) \quad (7)$$

where $Y(i,j)$ represents the blurred image, whereas $X(i+u, j+v)$ is the input image in which kernel matrix, $G(u,v)$, is applied.

3.2.3 Applying Morphological Operations

Morphology operations encompass image processing techniques based on the image shapes. These operations are instrumental in extracting hidden structures concealed within the images (Soille, 2000). The execution of a morphology operation utilizes the employment of several key terminologies, including structuring element, erosion, dilation, opening, and closing operations.

The structuring element is a matrix aiming to traverse the provided image, and its shape choice is one of the parameters that should be determined. Another significant term, erosion, seeks to shrink the image pixel by eroding the object's boundaries. During this process, if all the pixels in the structuring element cover the pixel of objects, these covered pixels are retained. Otherwise, object pixels are eliminated in the case of not fully matching the pixels. The mathematical operations to represent erosion can be seen in the following equation:

$$erosion = (A - B) \tag{8}$$

where A represents the input image while B is the structuring element. While the erosion operation creates more simplified object shapes, dilatation works reversely. Dilatation operation is liable to expand the object boundaries; in other words, it adds extra pixels to the outer part of the objects. The mathematical representation of this operation is:

$$dilation = (A + B) \tag{9}$$

While erosion and dilation operations reasonably impact images, their combination can also be utilized to achieve specific outcomes. One such combination, known as opening, involves the sequential application of erosion followed by dilation (10). On the other hand, the closing operation encompasses a dilation operation succeeded by erosion (11).

$$opening = (A - B) + B \tag{10}$$

$$closing = (A + B) - B \tag{11}$$

3.2.4 Canny Edge Detection Model

In computer vision applications, edge detection means discovering the properties of an object in an image. These properties aim to be discovered by detecting and characterizing significant intensity changes (Poletaev et al., 2016). Thus, essential edges and curves in the provided images can be detected. In the current phase of this study, the Canny Edge Detection method (Canny, 1986) were employed to extract the edges that represent electricity poles.

- Smoothing by Gaussian Convolution
- Gradient Calculation
- Process of Non-maximum Suppression
- Tracking of the Edges

In the first step of this edge detection model, Gaussian Smoothing (Gedraite & Hadad, 2011) is applied to eliminate the noises. After the blurring of the provided image, gradients are computed to detect the intensities and the directions of the edges, achieved through convolution with Sobel kernels (Kanopoulos et al., 1988) for both horizontal and vertical directions. This procedure facilitates the extraction of image edges; however, the intensity of these edges can exhibit variability. As a result, non-maximum suppression is applied, culminating in the thinning of edges. In the conclusive phase, the identification of strong and weak pixels representing the edges is determined, and a tracking algorithm selects the robust ones as the components of the edges.

3.2.5 Applying Line Segment Detector

The Line Segment Detector (LSD) developed by Von Gioi et al. (2012) is a computer vision algorithm designed to systematically analyze images to identify regions characterized by high edge density. These identified regions are subsequently merged to form coherent line segments. The functioning of the LSD algorithm

involves several key steps. An edge detector is initially applied to the images to identify edge points. Subsequently, the output from the edge detector undergoes a filtering process. This process involves the application of specific filters to the point data to generate hypotheses for potential line segments. These filters consider parameters such as the angle, length, and number of supportive points for each line segment hypothesis.

Following the generation of line segment hypotheses, a clustering algorithm based on proximity and similarity is employed. This clustering step serves to group related hypotheses by eliminating false positives. In the final stage of the LSD algorithm, a least-squares algorithm is utilized. This algorithm creates the line segment hypotheses by fitting them to the original edge points, which enhances the accuracy and precision of the extracted line segments.

3.2.6 Filtering the Detected Lines According to Its Length

Within this stage, the lines extracted via the Line Segment Detector undergo a length-based filtration process. Within the framework of the proposed method, lines possessing lengths below 50 pixels are excluded. This strategic elimination of shorter lines serves the purpose of discarding those unlikely to represent electricity poles accurately.

3.2.7 Extracting the Edges by Thresholding

This phase facilitates the preliminary extraction of edges by utilizing the extended lines generated in the preceding step. Within this segment, an algorithm is deployed to identify pixels that do not correspond to edges, encoding the values of these pixels as "1" by applying the "Draw Segments" function of the line segment detector. In the pursuit of extracting edges, a thresholding procedure is enacted, whereby pixel values surpassing the threshold of "1" are retained, while those below this threshold are disregarded.

3.2.8 Applying Hough Line Transform

Utilizing the Hough Line Transform (Duda & Hart, 1972) is instrumental in identifying straight lines, which accept edge maps as input. This methodology represents lines within the polar coordinate system, characterized by two parameters (r, θ). These parameters encapsulate the spatial location of a point, wherein the value of r indicates the distance from the origin, and the angle θ signifies the orientation relative to the polar axis (Figure 30).

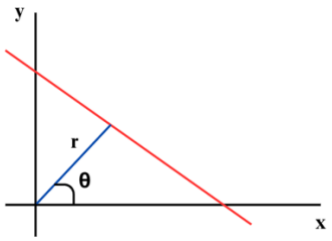

Figure 30. Polar Coordinate System

By using (r, θ) pair, line equation in Figure 29 can be written as:

$$y = \left(-\frac{cos\theta}{sin\theta}\right)x + \left(\frac{r}{sin\theta}\right) \quad (12)$$

The following equation (13) is obtained when this term is arranged. This equation means that for each point of (x, y), a family of lines that passes through this point can be described.

$$r = xcos\theta + ysin\theta \quad (13)$$

A family of lines can be obtained for all the points in an image, and if the curves of two points are intersected, these points are on the same line. As a result, the Hough Line Transform algorithm aggregates such intersecting points, thereby enabling the extraction of suggested lines.

3.2.9 Finding the Best Line That Represents the Electricity Poles

In the previous step, many lines are produced by the Hough Line Transformation. These line points are stored within a list, wherein the lines are ordered based on their prominence. Consequently, the optimal line that best represents the electricity poles is designated by selecting the initial element from the line list.

3.2.10 Measurement of the Tilt Angles of the Poles

All the gathered images exhibit a uniform rectangular configuration, ensuring that the angle between two adjacent boundaries of an image corresponds to 90 degrees. Utilizing this inherent property of the images, the determination of the angle between the representative line symbolizing the electricity poles and a vertical boundary line is facilitated within this phase. The steps of measuring the tilt angle of an electricity pole are demonstrated in the following equations:

$$degree = \theta * 180/3.14 \quad (14)$$

$$degree = \min(degree, 180 - degree) \quad (15)$$

In equation (14), the transformation from the polar to cartesian coordinates is applied, whereas equation (15) quantifies the inclination angle existing between the representative line and the vertical boundary of the image (Figure 31).



Figure 31. Representative Line and Vertical Boundary of the Image

3.3 Measurement of Performance Metrics

The image processing algorithm presented in the second section aims to estimate the representative lines corresponding to the electricity poles. To measure the accuracy of this algorithm, two distinct performance metrics, namely the Earth Mover's Distance (EMD) (Department et al., 1998) and the EA-score (Zhao et al., 2021), are employed. EMD is characterized as the measure of distance between two mathematical distributions, and according to Zhao et al. (2021), it can also serve as an indicator of line similarities. As a result, this similarity metric accomplishes this by (i) rasterizing the lines into pixels and (ii) computing the pixel-wise Euclidean distance, which is represented by the following equation:

$$distance = \sqrt{(x_1 - x_2)^2 + (y_1 - y_2)^2} \tag{16}$$

where (x_1, y_1) & (x_2, y_2) are coordinated two different points. The other metric, EA-score, proposed by (Zhao et al., 2021), utilizes Euclidean and Angular distances of two lines simultaneously. The following equation can measure the angular distance of two lines:

$$S_\theta = 1 - \frac{\theta(l_i, l_j)}{\pi/2} \tag{17}$$

where $\theta(l_i, l_j)$ represents the angle between two lines l_i and l_j. Furthermore, the Euclidean distance is described as:

$$S_d = 1 - D(l_i, l_j) \tag{18}$$

where $D(l_i, l_j)$ is defined as the Euclidean distance between two lines' midpoints. To measure the EA-score, angular and Euclidean distances are utilized as in the following equation:

$$S = (S_\theta * S_d)^2 \tag{19}$$

3.4 Risk Classification Method

Within the conclusive segment of the proposed model, the measured tilt angles are subjected to an examination following pre-established threshold values. This evaluation is conducted in alignment with the classifications of the poles. For instance, steel poles may inherently possess a structural inclination, whereas secure concrete and wooden poles are expected to maintain vertical standing (Figure 32). This necessitates the incorporation of distinct threshold values for steel and concrete-wooden poles.



(a) (b)

Figure 32. Representative Input Images for (a) Steel Pole, (b) Wooden Pole

The threshold value for a steel pole is established at 4 degrees. This value is derived from the summation of the natural inclination degree of a secure steel pole (3 degrees) and an error degree (1 degree), which is permissible within civil engineering standards. On the other hand, in the case of a concrete or wooden pole, the allowable inclination degree is limited to 1 degree, representing the extent of permissible error.

In this part of the study, measured inclination degree values of the poles are examined so that threshold values are not exceeded. In the case of excessing threshold values, the examining electricity poles are classified as “risky”. Otherwise, they are labeled as “not risky”.

CHAPTER 4

FIELD EXPERIMENTS

This chapter validates the proposed model for risk detection in tilted electricity poles through real-time image testing. During this phase, we selected a specific test region in Polatlı, Ankara, which featured electricity poles that were neither part of the training nor testing the object detection model. To assess the study's robustness and the high precision of its outcomes, we carefully selected several random road corridors within this test area, ensuring the presence of numerous steel, concrete, and wooden electricity poles.

Regarding the object detection model, we employed eight distinct shooting angles (1, 2, 3, 4, 5, 6, 7, 8) as illustrated in a representative schema (Figure 33). However, we used images acquired from angles 1, 3, 5, and 7 to measure tilt degrees. Representative images captured from these specific areas are presented in Figure 34.

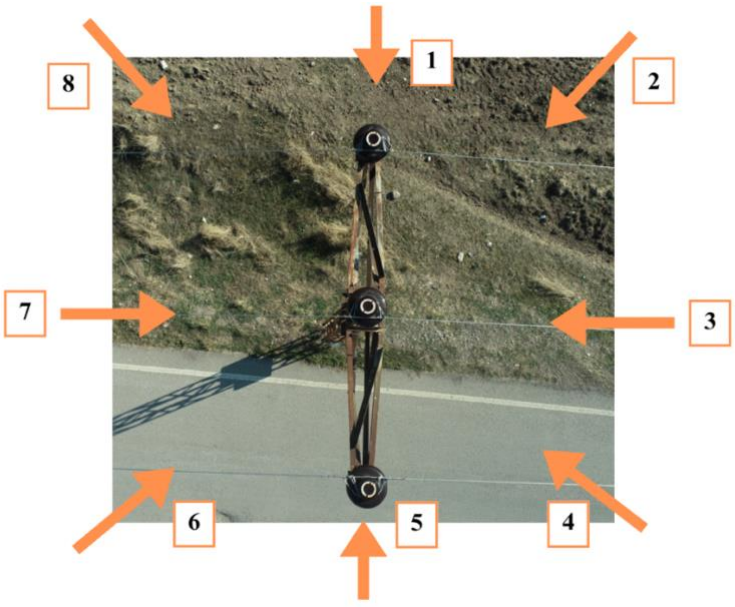

Figure 33. UAV Shooting Angles from Top View



Figure 34. Sample Images Collected from the Test Region

The data collection process was executed throughout these experiments using an UAV, specifically the DJI Mavic Pro 2. Noteworthy features of this vehicle are explained in the subsequent section. Its total takeoff weight, including the battery and propellers, is approximately 907 grams. The UAV can attain a maximum ascent speed of 5 meters per second, with a descent speed reaching 3 meters per second. Its operational altitude upon takeoff is restricted to 6000 meters, and the onboard battery sustains operation for a maximum duration of 31 minutes. The UAV boasts compatibility with both GPS and GLONASS satellite positioning systems.

Furthermore, it features a camera with a Field of View (FOV) spanning 77° and a focal length of 35 mm. This camera generates images with dimensions of 5472x3648 pixels and remains functional within a temperature range from -10°C to 40°C. Additional technical specifications are given in Table 2.

Table 2. Other Properties of DJI Mavic Pro 2 (DJI, 2023)

Aircraft	
Diagonal Distance	354 mm
Weight (Battery & Propellers Included)	907 g
Max Speed (near sea level, no wind)	72 kph
Maximum Tilt Angle	35° (S-mode, without remote controller)
Sensing System	
Sensing System	Omnidirectional Obstacle Sensing
Upward	Precision Measurement Range: 0.1 - 8 m
Sides	Precision Measurement Range: 0.5 - 10 m
Camera	
Sensor	1/2.3" (CMOS), Effective pixels: 12 million
Lens	FOV 83º 24 mm
Electronic Shutter Speed	8 - 1/8000 s
Photo	JPEG, DNG

During this study, images of electricity poles were acquired using UAVs equipped with cameras featuring a fixed gimbal angle of 45°. The consistent application of this gimbal angle ensures the uniformity of image properties across the dataset, thereby subjecting all pole images to the same evaluation conditions.

Under these specific conditions, the collection of electricity pole images took place at an approximate altitude of 19 meters, as illustrated in Figure 35. A total of 263 images of electricity poles were acquired for testing purposes within the Polatlı region under clear and sunny weather conditions. These collected images were subsequently transferred to a local computer, where the testing of the model commenced, employing this dataset that had not been previously utilized for training.

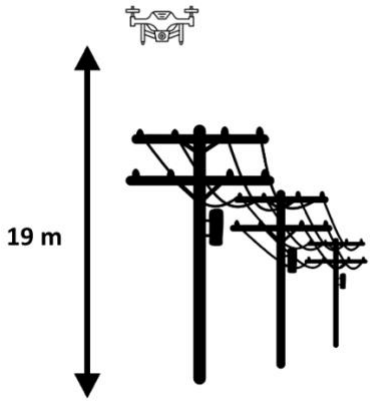

Figure 35. Approximate Altitude of UAVs Image Shooting

The unseen dataset were partitioned into two discrete subgroups: the initial subgroup encompasses images captured from shooting angles 1, 3, 5, and 7, whereas the second subgroup includes images obtained from shooting angles 2, 4, 6, and 8. The shooting angles with odd numerical designations detect the electricity poles, bounding box coordinate determination, and tilt degree measurement. Conversely, the images acquired from angles characterized by even numbers are exclusively utilized for the object detection model.

To evaluate the model's performance, 263 images collected from the Polatlı region were utilized for testing. Within this image set, those captured from shooting angles associated with odd numbers comprised 80 steel poles, 22 concrete poles, and 40 wooden poles. Conversely, the remaining images obtained from angles bearing even numerical designations encompassed 73 steel poles, 16 concrete poles, and 32 wooden poles. Notably, all the images are rendered in RGB color space and have a resolution of 5472x3648 pixels, aligning with the specifications of the UAV.

When subjecting all the images to testing using the proposed model, an assessment of the model's performance for validating the representative lines of the poles is conducted via two metrics: EMD and EA-score. These metrics are instrumental in establishing a similarity ratio between the ground truth and the detected

representative lines about electricity poles. The EMD value was 96.68 %, while the EA-score was 95.54 %.

During this testing phase, three distinct models were executed, each serving a specific purpose: the object detection model, advanced image processing techniques, and risk classification. In the initial object detection phase, the well-established Faster R-CNN deep learning model (Girshick, 2015) was employed to achieve precise and tightly localized bounding boxes encompassing the electricity poles. Following the object detection stage, a sequence of advanced image processing techniques was implemented to generate representative lines that convey the structural alignment of the electricity poles. These techniques include the application of Gaussian Blur, morphological operations, Canny Edge detection, Line Segment detection, the Hough Line Transformation, and a geometric rule for measuring the angle between two lines.

In the last phase, the risk status of the electricity poles was determined by assessing their inclination angles compared to predefined threshold limits. These threshold values are established by utilizing one of the outputs from the proposed object detector, specifically, the type of electricity poles. Given the distinct structural configurations of steel, concrete, and wooden poles, the imposition of unique threshold values becomes imperative.

During the evaluation of the risk status, a determination is made as to whether the measured tilt angles exceed the pre-established threshold values. The subsequent sections provide a comprehensive elaboration on the object detection model and the employed image processing algorithms

4.1 Object Detection Model

An advanced object detection model, Faster R-CNN, was employed in this study phase. The training of deep learning models heavily relies on the quantity and diversity of the available images. Consequently, a comprehensive dataset comprising

8775 images was meticulously collected using UAVs deployed in various regions across Turkey. These regions include Zonguldak, Bartın, Kastamonu, and Ankara.

As mentioned above, the substantial image dataset was instrumental in enhancing the training and performance of the object detection model. The acquisition of images from distinct regions enables the dataset to be at a desirable level of diversity. This diversity in the dataset provides a range of backgrounds upon the electricity pole images, which may include diverse elements such as automobiles, highways, pedestrian walkways, topographical features like mountains, and human figures. Furthermore, this approach introduces variations in lighting conditions that correspond to different weather scenarios, encompassing sunny and cloudy days. This diversity in the dataset effectively simulates real-world scenarios, thus enhancing the model's robustness and adaptability across various operational contexts.

Upon the conclusion of the data acquisition phase, which spanned approximately 60 days, meticulous labeling procedures were undertaken. The dataset was annotated with bounding box coordinates and the respective electricity pole types during this phase. These annotations were the foundation for training a supervised deep learning model, specifically Faster R-CNN. Before the training process, several pivotal considerations were meticulously conducted. These considerations encompassed the application of transfer learning methodologies, the employment of augmentation techniques, the selection of hyperparameters, and the selection of appropriate performance metrics. Subsequent sections explains these points mentioned above in detail.

4.1.1 Transfer Learning Method

The transfer learning method is used to initialize the deep learning model's weight vectors by utilizing previously trained models' weights, as mentioned in Chapter 3. Throughout this study, the object detection model's initialization was executed via

the utilization of the ImageNet dataset (Deng et al., 2010). This dataset comprises a substantial collection of over 1.2 million annotated images. The weight vectors that resulted from the training of the ImageNet dataset were utilized to initialize the object detection model.

4.1.2 Augmentation Techniques

Augmentation techniques expand the number of images by manipulating their inherent attributes. Within the scope of this study, a specific augmentation technique called “Random Flip” was employed, with a flip ratio of 0.5. Each input image is also resized to (800, 1333) dimensions. An example of the application of “Random Flip” can be seen in the following figure:



(a) Original Image



(b) Vertical Flip (c) Horizontal Flip

Figure 36. Sample Application of Random Flip

4.1.3 Hyperparameters

Hyperparameters are the parameters set before the training of a deep learning model, and they control the learning process. Throughout the training phase of the proposed object detection model, a selection of hyperparameters and their corresponding values are indicated in the subsequent table.

Table 3. Hyperparameters and their proposed values

Learning rate	0.002
Batch size	2
Optimizer	Stochastic Gradient Descent
Momentum	0.9
Weight Decay	0.0001
Epoch number	15
Loss Function	Cross-Entropy Loss

4.1.4 Performance Metrics

Performance metrics are instrumental in assessing the efficiency of electricity pole detection. In this study, precision and recall metrics were employed to quantify performance. The evaluation of these metrics entails the consideration of terms concerning the identification of positive and negative instances. These terms are explained in the following table:

Table 4. Description of the performance metrics' terms

True Positive	How many times did the model **correctly** classify a *Positive* sample as *Positive*?
False Negative	How many times did the model **incorrectly** classify a *Positive* sample as *Negative*?
False Positive	How many times did the model **incorrectly** classify a *Negative* sample as *P*ositive?
True Negative	How many times did the model **correctly** classify a *Negative* sample as *Negative*?

Precision measures the accuracy of the proposed model in classifying a sample as positive, whereas the model's ability to detect positive samples can be obtained by Recall. The equations of these metrics can be represented with the following formulas:

$$Precision = \frac{True\ Positive}{True\ Positive + False\ Positive}$$

$$Recall = \frac{True\ Positive}{True\ Positive + False\ Negative}$$

4.1.5 Training Object Detection Model

The proposed Faster R-CNN object detection model that utilizes ResNet50 with FPN (r50 FPN) as a backbone structure, i.e., Faster R-CNN r50 FPN is trained for 50 epochs. An early stopping rule were implemented to ascertain the optimal number of epochs, which evaluates whether three consecutive changes in loss differences are less than 0.001. According to this rule of thumb, the final epoch number were decided as 15. Throughout model training, following the common practice (Chen et al., 2019), the learning rate is kept constant until the ninth epoch, then divided by ten at the beginning of the 9th and 11th epochs.

The images are partitioned for training purposes with a training-test ratio of 0.8 to 0.2. Consequently, the training dataset comprises 5460 steel, 1484 concrete, and 68 wooden pole images, while the test dataset consists of 1381 steel, 364 concrete, and 18 wooden pole images.

After the training process has terminated, the training loss curves of the object detector are given in Figure 37.

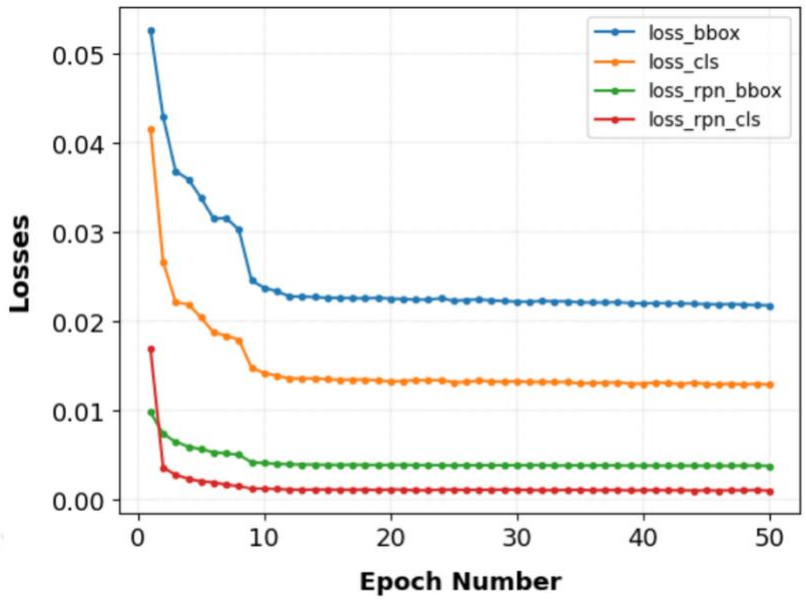

(a)

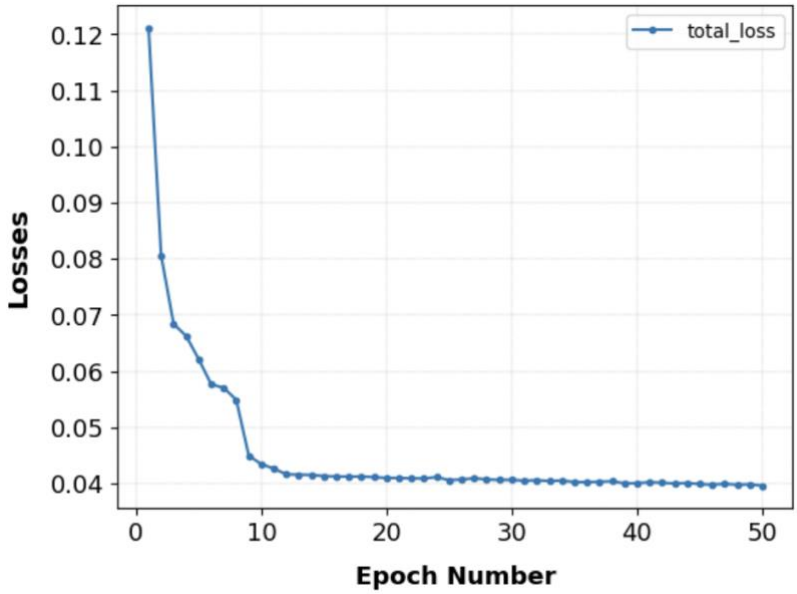

(b)

Figure 37. The Loss Curves of Faster R-CNN Object Detector (a) Separate losses and (b) Total loss

After the training process is terminated, the final values for the precision of the proposed model are obtained in the Table 5:

Table 5. Detection results of the proposed object detector

	Precision (%)	Average Precision (%)
Steel Pole	97.7	94.4 (IoU=0.5)
Concrete Pole	95.6	
Wooden Pole	89.8	

Precision-Recall figures are provided to comprehend the model's strength using precision results to comprehend the strength of the model by utilizing precision results.

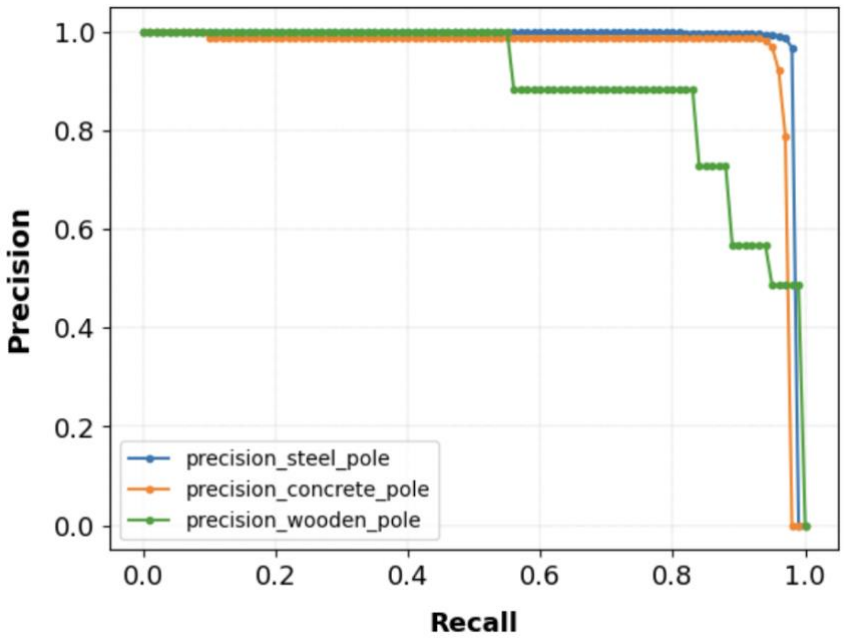

(a)

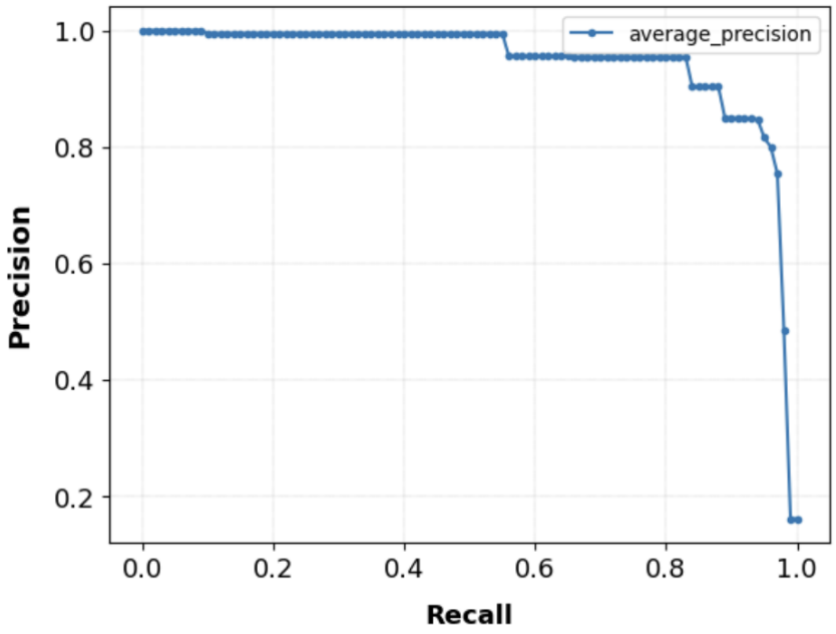

(b)

Figure 38. Precision-Recall Curves (a) Classwise (b) Average Precision

The Precision-Recall (PR) curves serve as a means to evaluate the efficacy of the proposed model, as they allow for a comparison of the area under the curves (AUC). An analysis of the classwise PR curves reveals that the steel pole detection exhibits the highest precision outcome compared to concrete and wooden poles, as evidenced by the higher AUC value. Conversely, the class of wooden poles emerges as the least successfully detected, which aligns with expectations given the lower number of images containing wooden poles compared to other pole types. Some output images of the proposed object detector are given in Figure 39.



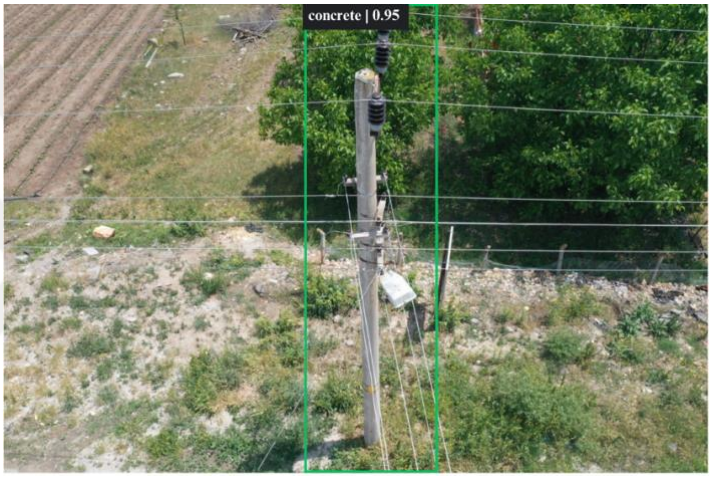

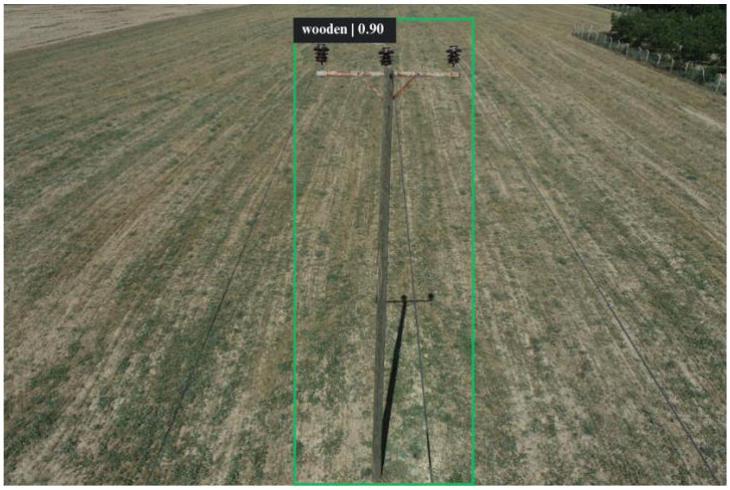

Figure 39. Output Image Samples of the Object Detector

4.2 Image Processing Algorithms

In the second phase of the proposed approach, a series of image-processing techniques are applied. These techniques leverage the outcomes of the object detector, precisely the bounding box coordinates of the electricity poles, to facilitate the extraction of the target objects from the images. Consequently, smaller-scale images containing the electricity poles and reduced-size elements from the surroundings are obtained. These cropped images are subsequently fed into the sequence of image processing techniques. In the forthcoming sections, the outcomes obtained from each step of the proposed algorithms are provided.

- Converting RGB image to Grayscale images

  After this conversion is applied to the sample images from the dataset, the following results are obtained (Figure 40):

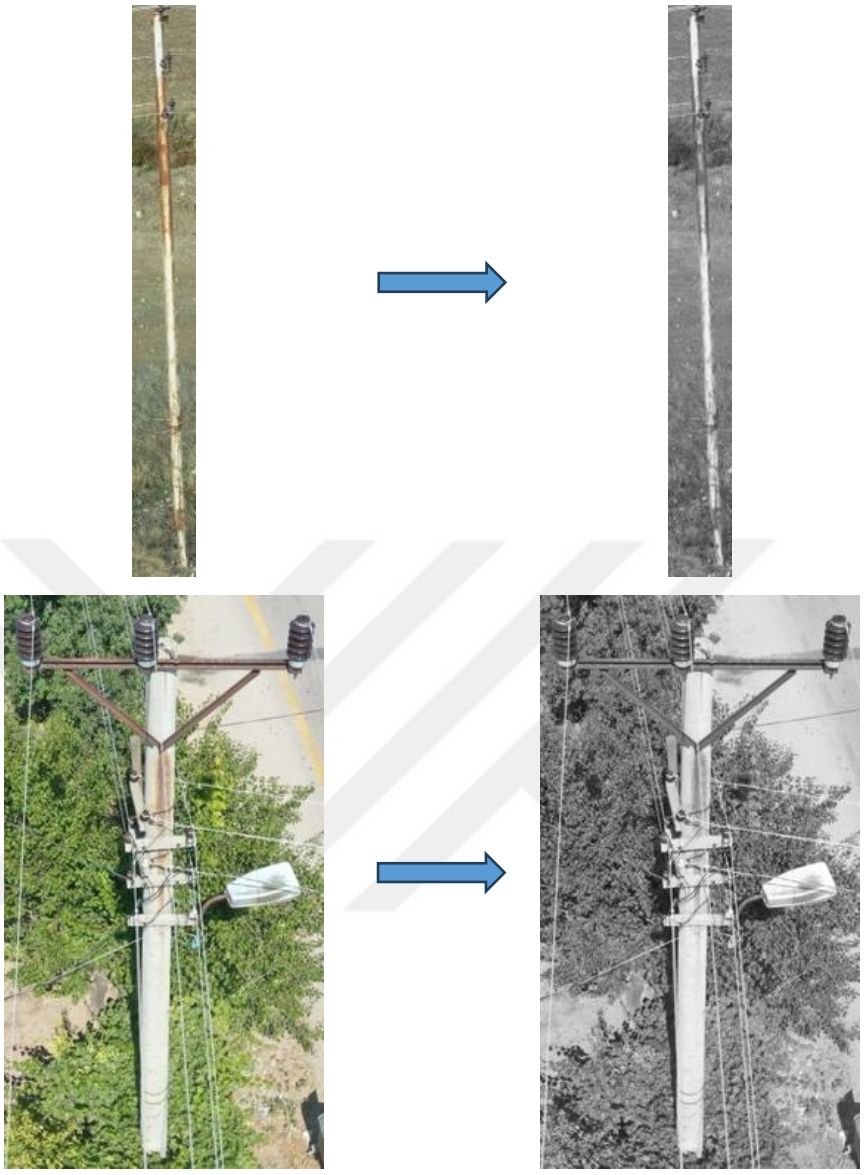

Input Images *Images in Grayscale*

Figure 40. Converting Cropped Images to Grayscale

- Applying gaussian blur

After the convolution process involving a 15-by-15 kernel, the resulting output images are depicted in the forthcoming figure (Figure 41). This step aims to mitigate the presence of minor image noise artifacts, thereby enhancing image clarity.

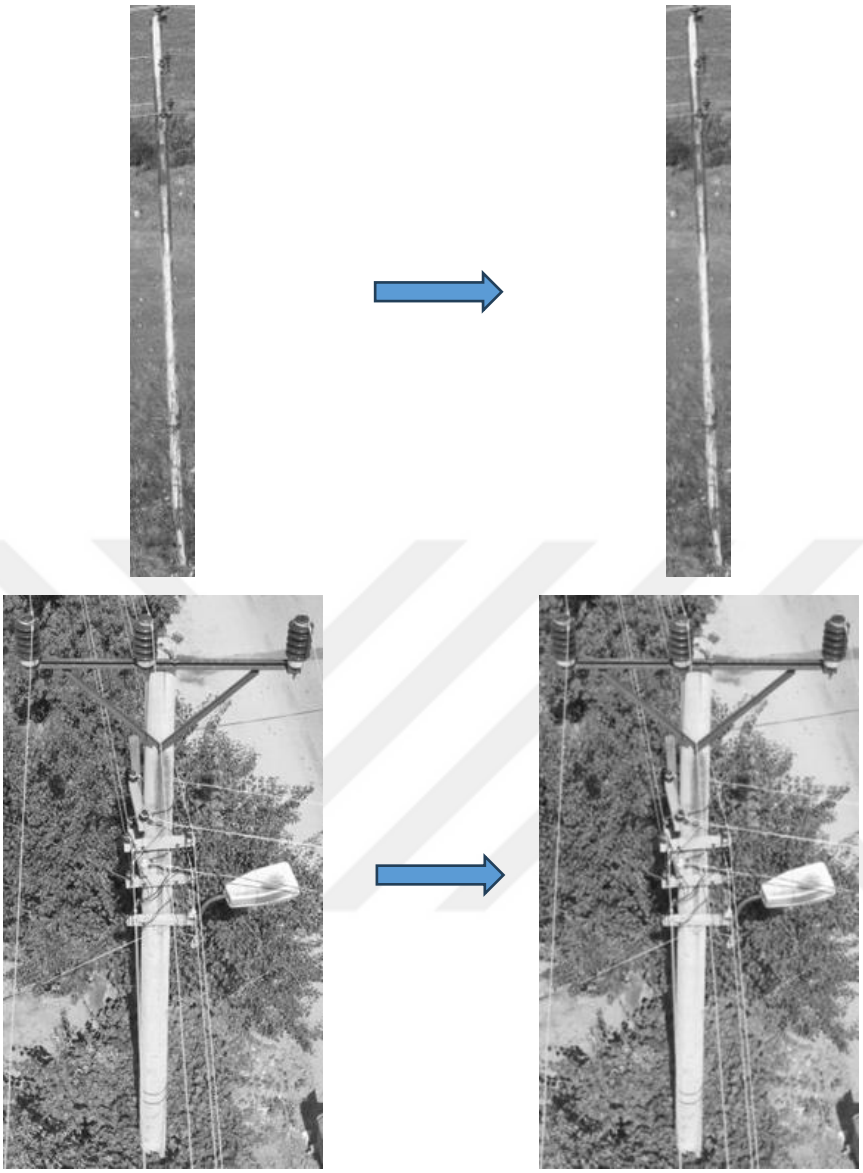

Input Images *Blurred Images*

Figure 41. Applying Gaussian Blur to Input Grayscale Images

- Applying morphological operations

In this phase, the previously obtained blurred images from the second stage are employed as input. During this step of the study, a series of morphological opening operations, combined with a single erosion operation, are executed using a structural element of a 25-by-25 ones-matrix. These operations are undertaken

to remove undesired objects, such as cars, highway lines, and houses, from the images. The outputs produced following this step are given in Figure 42.

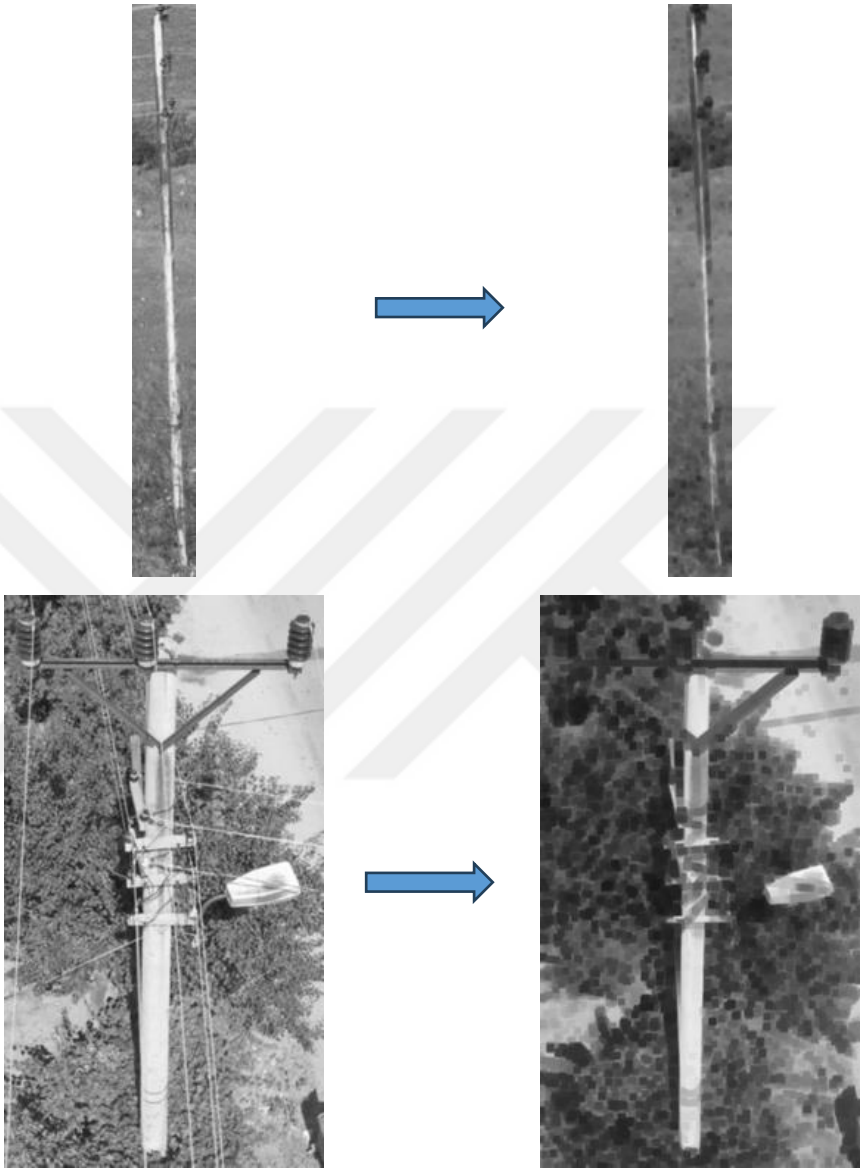

Input Images *Output Images*

Figure 42. Applying Morphological Operations to Input Images

- Utilizing the Canny Edge Detection Model

Following applying the Canny Edge Detector with specified parameter values, including a low threshold of 10, a high threshold of 200, and an aperture size of

5, the resultant output images are illustrated in Figure 43. This phase is designed to identify and delineate the prominent edges of objects within the images.

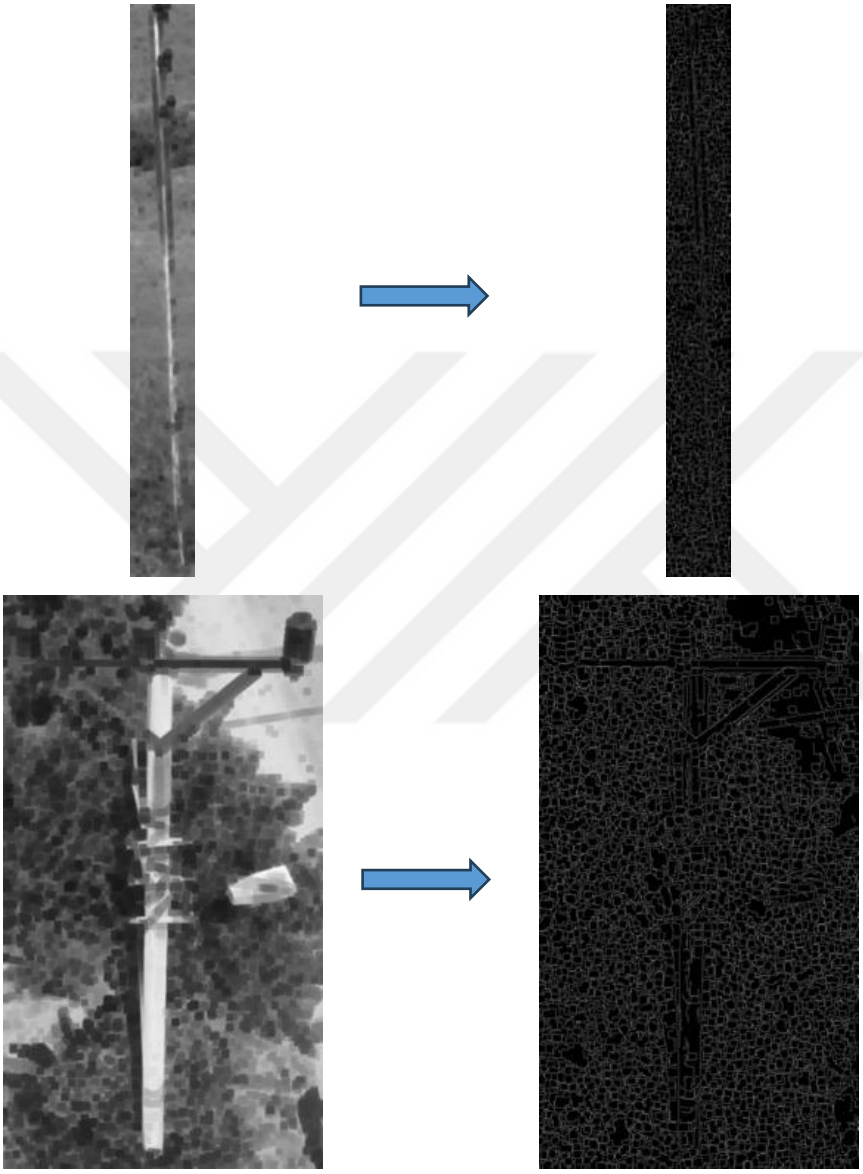

Input Images *Output Images*

Figure 43. Applying Canny Edge Detector to Input Images

- Application of Line Segment Detector, Filtering Detected Lines and Thresholding

During this stage, the line segment detector is deployed to identify prominent linear segments within the images. After detecting these line segments, a filtration procedure is implemented to eliminate shorter segments less likely to represent electricity poles effectively. This filtering process employs a predetermined threshold of 50 pixels as a length constraint. Following the sequential execution of the line segment detection, long line filtration, and thresholding operations, the resultant output images are presented in Figure 44.

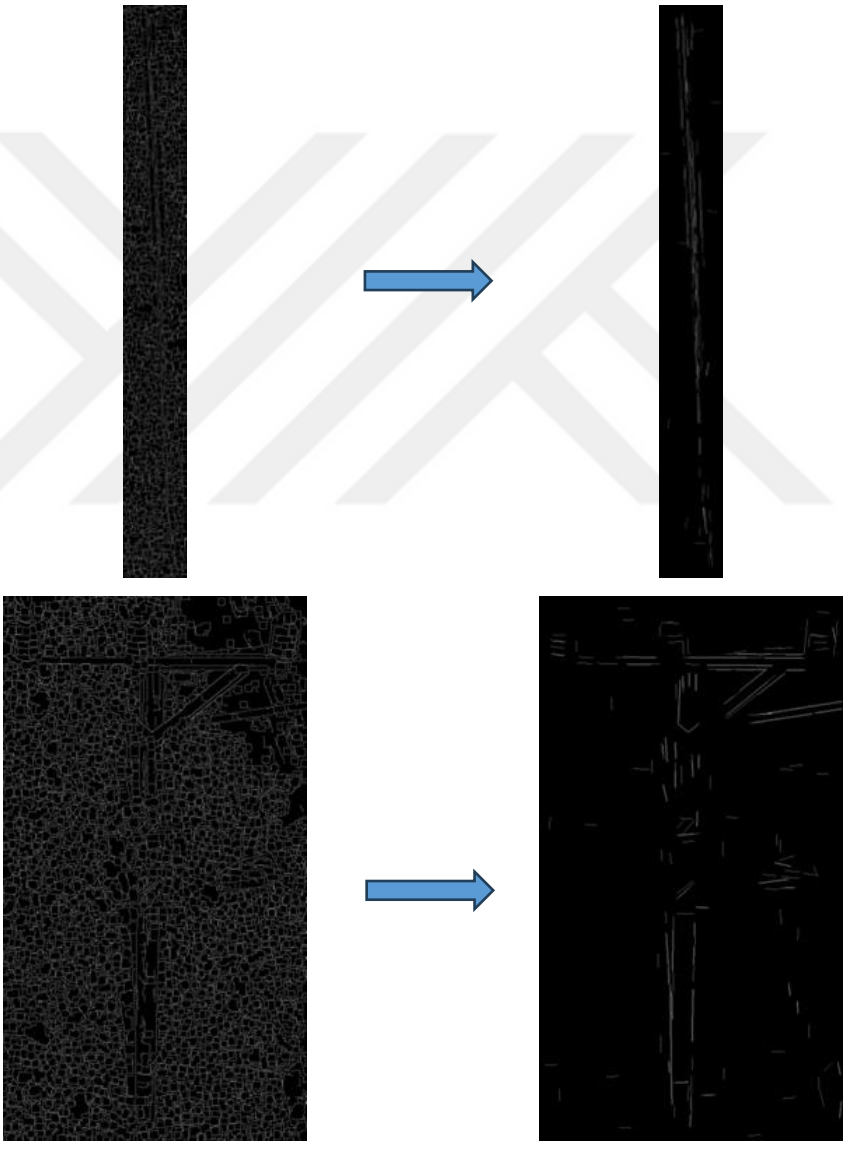

Input Images *Output Images*

Figure 44. Representation of Extracted Edges

- Applying Hough Line Transform

In this phase, candidate lines potentially indicative of electricity poles are discerned by applying the Hough Line Transformation. This procedure inputs the edge maps derived from the preceding edge detection stage. This algorithm's application to the edge map acquired in the previous step yields the delineation of lines overlaid on the original images, as exemplified in Figure 45.

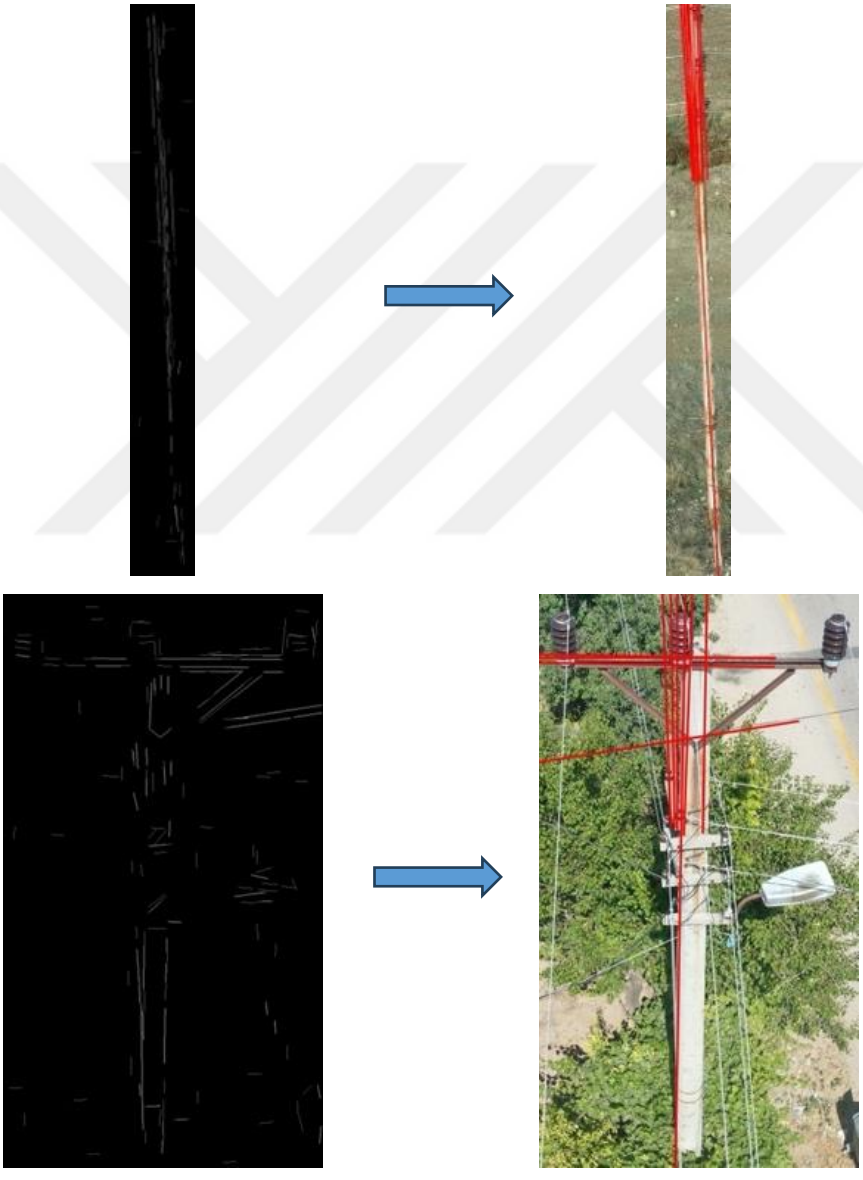

Input Images *Output Images*

Figure 45. Proposed Lines by Hough Line Transformation

- Finding the Best Line That Represents the Electricity Poles

The Hough Line Transformation employs a voting algorithm to identify the most prominent line that signifies the presence of electricity poles. Consequently, each candidate line generated through this transformation accrues a certain number of votes based on the underlying algorithmic mechanism. The line with the highest vote count is the optimal representative line for the electricity poles. An illustrative demonstration of the process for selecting the best line is presented in Figure 46.

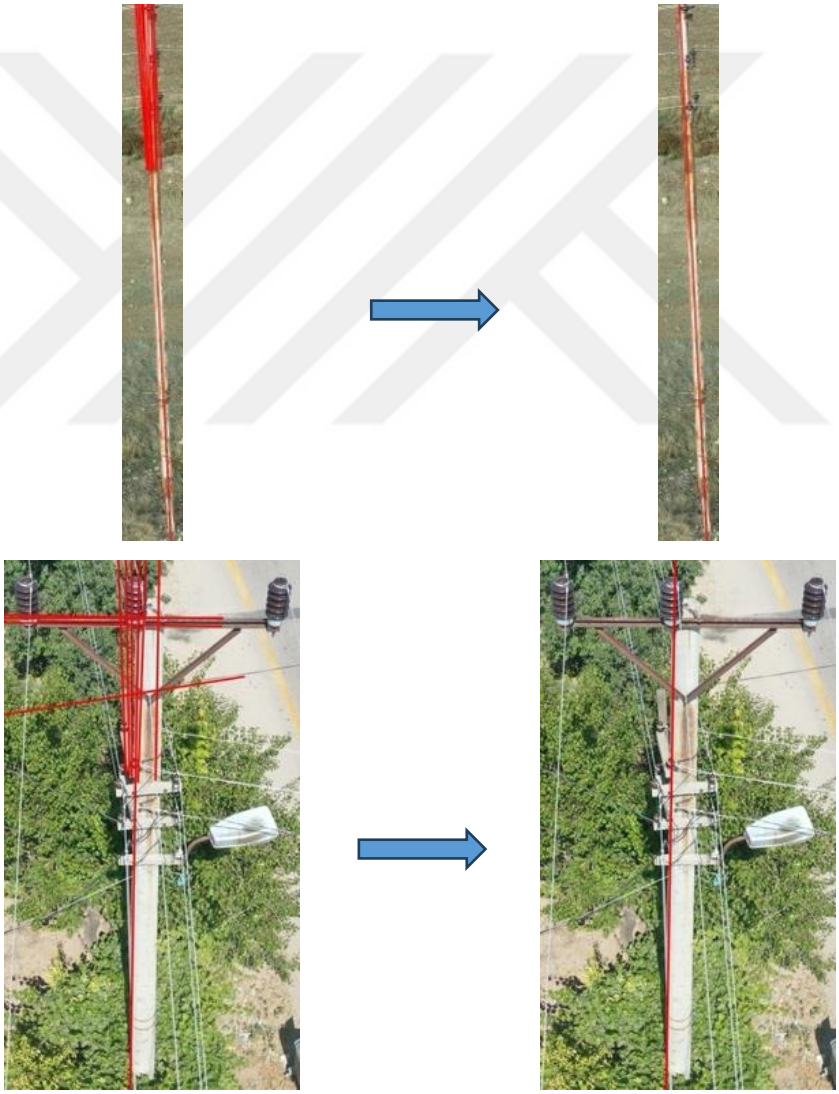

Input Images *Output Images*

Figure 46. Selecting the Best Line

- Measurement of Tilt Angles of the Poles

In the concluding segment of the image processing algorithms, the tilt angle of the electricity poles is determined. In this phase, a hypothetical vertical line parallel to the vertical edge of the image serves as the reference line. When measuring the tilt angles of an electricity pole, the angle between the reference line and the detected representative line is calculated. The measurement procedure is visually elucidated in Figure 47.



Figure 47. Example Measurement of Tilt Angle

4.2.1 Validation of the Representative Lines

The primary objective of the proposed algorithm is to generate representative lines for electricity poles. It is essential to validate the generated representative lines to assess the robustness and accuracy of this algorithm. Therefore, a meticulous labeling procedure is undertaken to measure the algorithm's accuracy and ability to produce accurate representative lines.

In the labeling process, 592 images obtained from shooting angles 1, 3, 5, and 7 (as depicted in Figure 30) were meticulously labeled using the Labelme software (Russell et al., 2007). The labeling endeavor required a collective effort equivalent to 4.11 hours per person. Upon completion of the labeling phase, the accuracy of the algorithm's generated representative lines was assessed by applying two

performance metrics: EMD and EA-score. These metrics quantify the degree of similarity between the truth and detected lines. The outcomes of these evaluation metrics are tabulated in Table 6.

Table 6. Results of the Performance Metrics

Earth Mover's Distance (%)	98.56
EA-score (%)	95.95

The observed unity between the detected representative lines and the ground-truth data is the robustness of the algorithm proposed. The noteworthy levels of success, as evidenced by the auspicious matching values presented in Table 6, substantiate the model's capacity for detecting representative lines associated with electricity poles and accurately measuring their tilt angles with a commendable degree of accuracy.

4.3 Risk Classification

In the final segment of this investigation, the classification of risk for individual electricity poles is achieved by applying class-specific thresholds. Considering the inherent structural inclinations of steel poles, an allowable inclination angle of 4° is established. In contrast, concrete and wooden poles are subject to a threshold of 1°.

The classification of poles according to their inclination angles is represented in Figure 48. Among the overall count of 409 steel poles, 237 are classified as "Not Risky". Similarly, out of 171 concrete poles, 65 fall under the "Not Risky" category. Four of the 12 wooden poles are classified as "Not Risky".

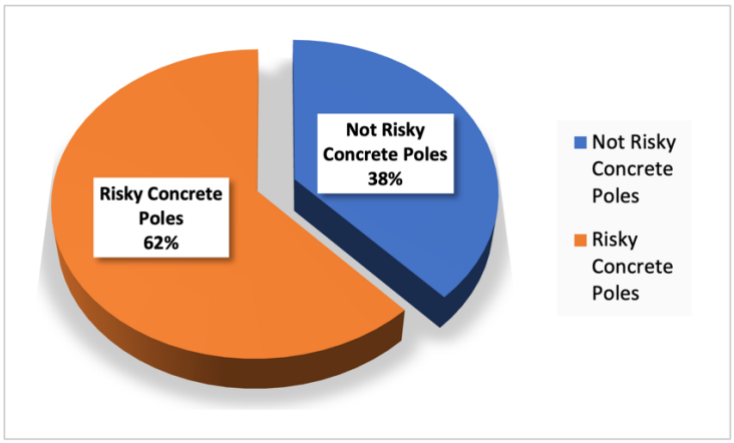

(a)

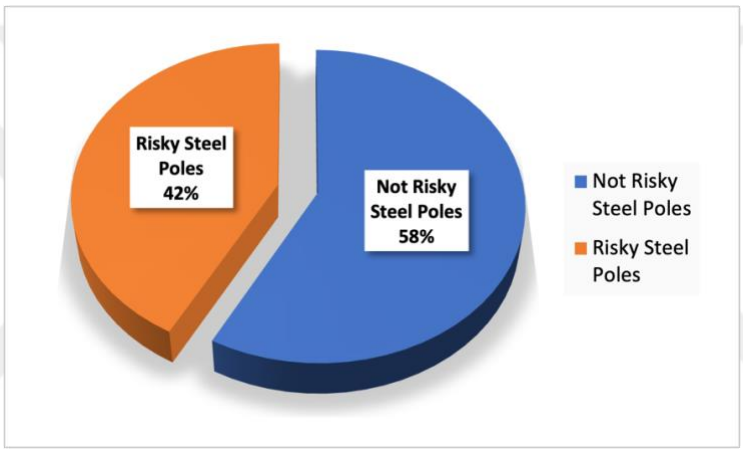

(b)

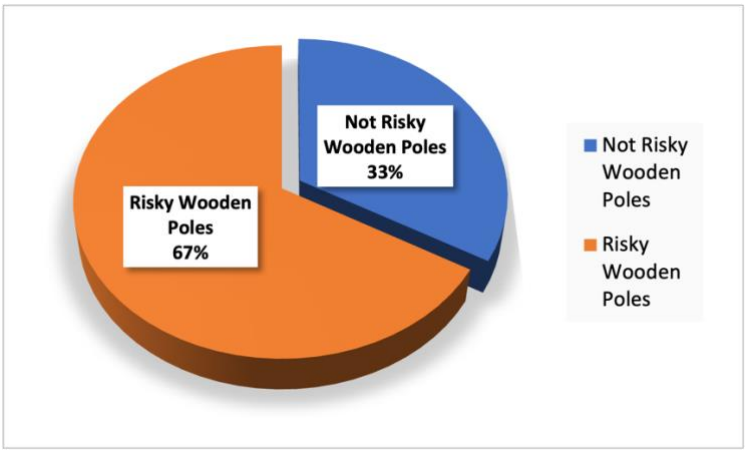

(c)

Figure 48. Risk Classification Results of the Electricity Poles (a) Concrete Pole, (b) Steel Pole and (c) Wooden Pole

Some output images of the proposed model are indicated in Figure 49.

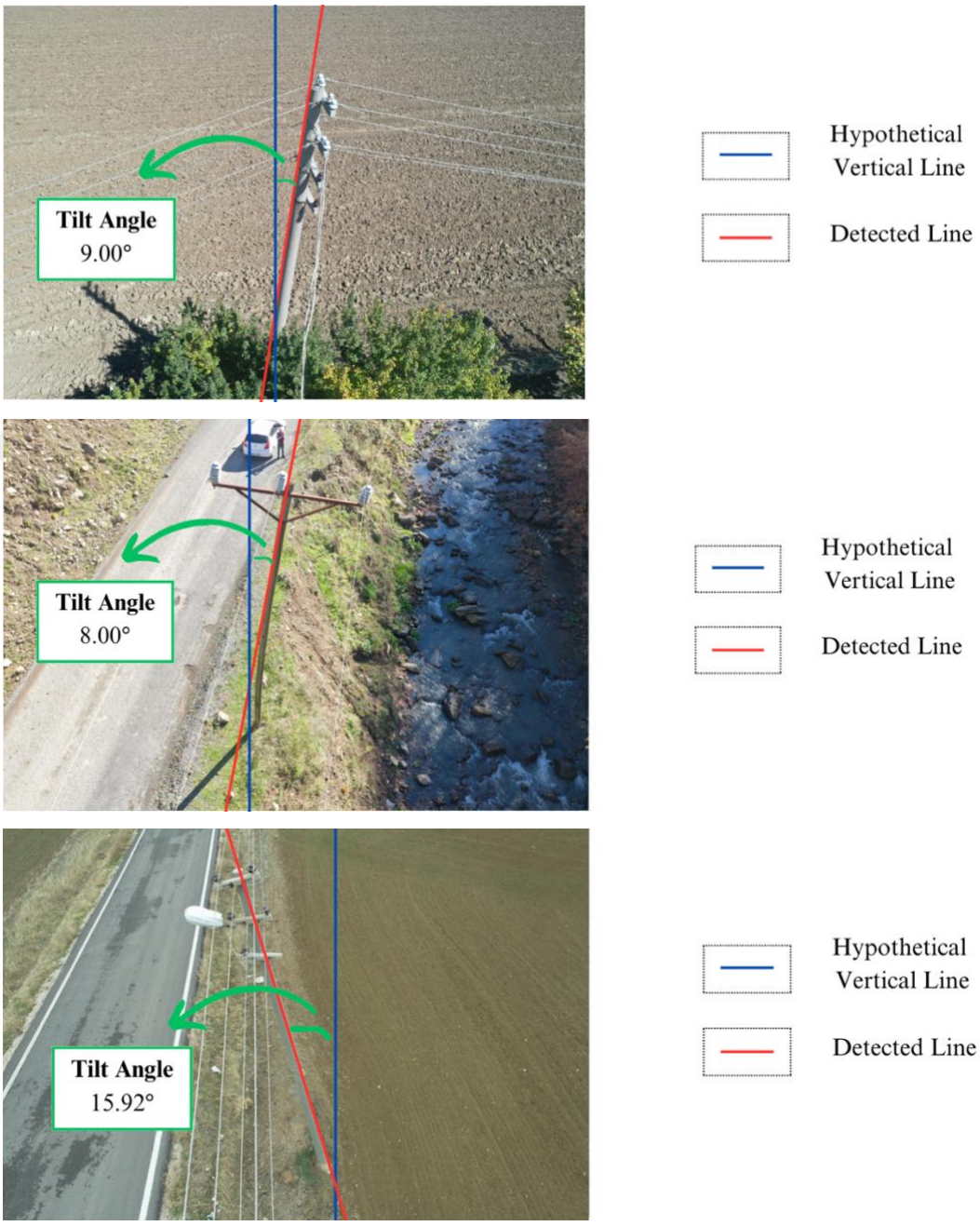

Figure 49. Output Images from The Proposed Model

4.4 Results and Discussion

The performance of the proposed risk classification model has been illustrated in the preceding sections. Based on the outcomes derived from the object detection model, image processing algorithms, and the risk classification model, it is observed that the proposed model exhibits a remarkable ability to classify the risk associated with tilted electricity poles. This notable capability is primarily attributed to acquiring an extensive dataset comprising real electricity pole images. It is a common practice that an increase in the volume of data results in a proportional enhancement of the robustness of artificial intelligence models (Zhou, 2016). In conjunction with many datasets, the diversity of these images assumes paramount importance, allowing for incorporating various natural environmental conditions during the training phase.

This study systematically collected 8,775 electricity pole images over 60 days. These images were procured from diverse regions across Turkey, encompassing locations such as Ankara, Bartın, Kastamonu, and Zonguldak, utilizing UAVs. Noteworthy aspects of this data collection phase include (i) acquiring real electricity pole images and (ii) implementing structured data collection methods.

The significance of collecting real images is highlighted by the findings in the existing literature, where studies have relied on simulated electricity pole images to train risk classification models for tilted utility poles. For example, in the work of Chen and Miao (2019), an artificial dataset of electricity pole images was generated for training a deep learning model to detect hazardously tilted electricity poles. While their study aimed to simulate a dataset that included environmental elements such as buildings located behind the poles, it did not faithfully replicate real-life scenarios. In contrast, this present study features a diverse array of actual environmental objects within the collected images (Figure 50), thereby providing a more realistic foundation for the proposed risk classification model.



Figure 50. Images Including Various Types of Environmental Objects

Furthermore, certain existing studies in the literature have relied on images sourced from Google Street views (Lin et al., 2017) and satellite imagery (L. Li et al., 2021). While these image collection methods aim to incorporate real electricity pole images, they often lack the utilization of well-structured image shooting angles. Additionally, the inherent limitations in resolution within satellite images can lead to poorly trained deep learning models, resulting in less reliable risk classification outcomes.

In contrast, for the training procedure of the proposed model, UAVs were deployed to acquire high-quality and high-resolution images of electricity poles, employing efficient and expeditious methods. During the data collection process in this study, four images were captured from each of the four sides of the electricity poles, all from a close point of view and directly aligned with the poles (Figure 51). This approach facilitates a highly precise and reliable method for measuring tilt degrees.



Figure 51. Images Collected for the Detection of Tilted Electricity Poles

After the training phase of the object detection model, it yielded average precision values of 97.7%, 95.6%, and 89.8% for steel, concrete, and wooden poles, respectively. These average precision values suggest that the proposed model's capacity for detecting wooden poles is comparatively less successful than its performance with steel and concrete poles. This difference can be primarily attributed to the limited number of available wooden pole images compared to the substantial number of steel and concrete pole images. Consequently, there are instances where wooden pole images may be erroneously classified as concrete poles (Figure 52). Nevertheless, the mean average precision value achieved by the object detection model, 94.4%, exceeds the performance metric results reported in similar studies within the existing literature.



Figure 52. Incorrectly Classified Wooden Pole

Another noteworthy consideration is detecting the shadows of the electricity poles (Figure 53), which can potentially lead to inaccuracies in tilt angle measurement. Given that most of the images in the dataset were captured under sunny weather conditions, it is plausible for the shadows of utility poles to be present on the images. To mitigate this issue, a meticulous and comprehensive labeling procedure was executed. This procedure involved drawing sufficiently tight and compact bounding boxes, including all segments of the electricity poles. Such an approach effectively eliminates the influence of shadows cast by the utility poles during the training phase. Consequently, the proposed model is trained using labels representing the actual locations of the electricity poles, thereby enhancing its accuracy.



Figure 53. Images Including Shadows of the Electricity Poles

The output generated by the object detector was employed to crop the images, and this cropped data was subsequently utilized as input for a series of image processing techniques. These techniques were employed to identify a line that accurately represents the structural alignment of the electricity poles, facilitating the measurement of the poles' tilt angles. A notable contribution of the proposed method lies in its incorporation of a validation process for the detected representative lines and the utilization of geometric principles for measuring the inclination angles of the poles.

A rigorous labeling procedure was executed to ascertain the validity of the representative lines, and two performance metrics quantified the similarity ratio between the truth and the detected lines. This validation process constitutes a pivotal contribution, as it furnishes quantitative outcomes for detecting the representative lines. The measured values for these metrics were 98.56% for the EMD and 95.95% for the EA-score, signifying that the proposed model consistently generates highly accurate representative lines.

While the performance metric results are highly successful, particular challenges remain associated with detecting representative lines. Once the images are cropped, utilizing the bounding box coordinates derived from the object detector, the primary objective is to mitigate environmental interferences, such as vehicles, buildings, and trees. This approach can remove most environmental objects; however, it is important to note that certain essential elements, such as electricity cables and road markings, cannot be eliminated.

Consequently, electricity cables and road markings within the cropped images can occasionally lead to their misidentification as electricity poles (Figure 54), yielding inaccurate tilt angle measurements. To address this issue, morphological operations with larger kernels are implemented. These operations effectively remove road markings and electricity cables from the images. While applying morphological operations, it is noteworthy that only 16 out of 592 images were misclassified, underscoring the robust performance metrics exhibited by the proposed method.



(a) (b)

Figure 54. Misidentified Lines (a) Electricity Cable, and (b) Road Markings

Furthermore, determining the poles' tilt angles is accomplished by measuring angles between two lines. The utilization of fundamental geometric principles for angle measurement yields reliable and comprehensible results, thereby enhancing the efficacy of the risk classification model.

CHAPTER 5

SUMMARY, CONCLUSIONS, AND FUTURE WORK

5.1. Summary

Regular maintenance, surveillance operations, and risk assessments for the electricity line corridors are imperative to ensure continuous power supply. These responsibilities predominantly rely on human personnel such that they have to conduct a manual control and repair cycle to patrol through electricity corridors and detect possible anomalies. However, this manual cycle demands a substantial workforce and carries the potential for errors. This highlights the emergent requirement to explore autonomous and efficient methods for accurately surveilling electricity poles to identify possible anomalies.

As a result, this research deals with a specific anomaly that presents potential risks: the insecure tilting of electricity poles. Such tilts can lead to energy losses and pose collapse hazards and suspension of electricity lines, warranting immediate attention. To address this concern, artificial intelligence applications, along with advanced image processing algorithms, are utilized.

This study uses a risk detection model to capture various electricity pole images utilizing UAVs. A total of 8775 electricity pole images with various backgrounds were collected from different regions during the data collection procedure.

Within the risk detection framework, an object detector, Faster R-CNN, is integrated to precisely recognize and classify the electricity poles using bounding boxes. Additionally, some image processing techniques, including blurring, morphological operations, Canny edge detection, Line Segment Detector, and Hough Line Transform, are employed to measure the tilt angle of each pole. Based on these

angles, the electricity poles are classified as ‘risky’ or ‘not risky’ related to their structural integrity and stability.

Labeling operations provide annotated inputs for object detection and risk classification methods to maintain this procedure. The output values of the object detectors are employed to crop images for subsequent processing. Furthermore, representative tilt lines are obtained after applying several image processing techniques to the crop images. These lines' accuracy is validated using performance metrics to comprehend the matching scores. Furthermore, a testing area in Polatlı, Ankara, was meticulously chosen to authenticate the proposed model's performance. A comprehensive dataset comprising 263 images of electricity poles was collected from this specific region to assess the model's robustness against an unseen dataset.

The study illustrates the substantial efficiency of the proposed risk assessment model, achieving noteworthy accuracy, precision, and recall metrics. Consequently, this model holds considerable potential for the practical identification of risks associated with electricity poles, significantly contributing to the dependability and safety of power distribution systems.

5.2. Conclusions

This study presents an innovative approach for classifying risk associated with tilted electricity poles, utilizing UAVs. The proposed model consists of three distinct components: (a) an Object Detection Model, (b) a series of image processing techniques, and (c) a Risk Classification Method. This method facilitates the identification of tilted electricity poles by utilizing the capabilities of the robust object detection model, Faster R-CNN, alongside estimating tilt angles and subsequent risk classification. Within the framework of the object detection model, the algorithm is designed to detect and classify three classes of electricity poles: Concrete, steel, and wooden poles.

The proposed multi-stage risk classification method exhibits exceptional proficiency in detecting, classifying, and quantifying the tilt degrees of electricity poles by utilizing RGB images. An interesting observation was made upon validation of the object detection algorithm: wooden poles sometimes exhibited misclassification as concrete poles despite accurately estimating their bounding box coordinates. This particular misclassification is unsurprising, as the structural forms of these two pole types are very familiar. The primary differentiating factor is the poles' section areas, with concrete poles generally having larger sections.

Moreover, a variety in color exists between these pole types, although such distinctions may not be apparent on sunny days. In light of these details, the precision values for the detection outcomes of steel, concrete, and wooden poles are obtained as 97.7%, 95.6%, and 89.8%, respectively. These results are very reasonable and successful for a UAV-based object detection algorithm.

The tilt angle classification method relies on the bounding box coordinates generated by the object detector to extract the electricity pole, followed by applying a sequence of image processing algorithms. This phase of the study presented a significant challenge in identifying the representative lines of the electricity poles, with the primary source of noise electricity lines. Sometimes, these electricity cables could be erroneously detected instead of the poles. The sequence's order was devised to address this issue. After representative lines for the electricity poles are detected, the alignment accuracy between the detected and actual lines is measured, and two performance metrics are employed.

The metrics of EMD and EA-Score yield values of 98.56% and 95.95%, respectively. These outcomes strongly suggest that the primary challenge of potential misdetection of electricity cables were addressed, and the sequence of image processing algorithms exhibits remarkably high performance.

After successfully detecting representative lines for the electricity poles, the subsequent step involves measuring the inclination angles using geometric principles. High and successful matching ratios between truth and detected lines also

indicate a high accuracy for the measurement of tilt angles of the electricity poles. The risk classification process is then executed by considering allowable inclination angle thresholds corresponding to the electricity pole class types.

Upon validation of the proposed model using an unseen dataset obtained from Polatlı, Ankara, an average similarity ratio of 96.11% is attained. This notable matching ratio is a compelling testament to the robustness and credibility of the proposed model.

Despite the numerous advantages of the proposed method, several challenges still need to be addressed. One significant challenge arises that most images were acquired under daylight conditions, potentially leading to reduced performance when faced with varying weather conditions. Moreover, image collection via UAVs can become challenging during adverse weather conditions such as wind or rain. In addition to the challenges related to image acquisition, implementing a real-time risk classification method could offer more efficient solutions by minimizing the waste of time transferring images from the sites to computing facilities.

5.3. Future Work

The proposed model must constitute a fully automated method for classifying risk associated with tilted electricity poles. As a result, the following subject matters can be further investigated in the future:

- While there exists a variety of classes of types of electricity poles, this study has focused explicitly on steel, concrete, and wooden poles. In forthcoming research, including images from high-voltage poles could also contribute to a diverse dataset.
- Due to the diverse shapes of steel poles, the current risk classification method might not indicate optimal performance. Given that the natural inclination degree of steel poles can vary based on their specific types, assigning different allowable inclination limits becomes necessary. To address this,

images of different kinds of steel poles can be collected, accompanied by the training of more sophisticated object detection models.

- Varying weather conditions can influence images' contrast, brightness, and hue; therefore, this variability in lighting conditions should be considered. To enhance the model's robustness, images captured during different seasons, each characterized by distinct lighting conditions, can be added to the training dataset.
- During this study, the focus has been on one specific anomaly type that can occur on electricity poles. Future research could study various anomaly types, including investigating issues like birds' nests, vegetational encroachment, and broken/rusted insulators.
- This study has utilized images acquired through UAVs for analysis. However, other image collection platforms that offer superior image quality could enhance the performance of the proposed models.
- During this study, images were collected on-site and then transferred to servers to apply the proposed model. Investigating real-time anomaly detection directly on electricity poles could be explored to mitigate the waste of time caused by image transfers.

REFERENCES

Ahmad, J., Malik, A. S., Abdullah, M. F., Kamel, N., & Xia, L. (2015). A novel method for vegetation encroachment monitoring of transmission lines using a single 2D camera. Pattern analysis and applications, 18, 419-440.

Blaabjerg, F., Teodorescu, R., Liserre, M., & Timbus, A. V. (2006). Overview of control and grid synchronization for distributed power generation systems. IEEE Transactions on industrial electronics, 53(5), 1398-1409.

Canny, J. (1986). A computational approach to edge detection. IEEE Transactions on pattern analysis and machine intelligence, (6), 679-698.

Chen, B., & Miao, X. (2020). Distribution line pole detection and counting based on YOLO using UAV inspection line video. Journal of Electrical Engineering & Technology, 15, 441-448.

Cracknell, A. P. (2007). Introduction to remote sensing. CRC press.

Department, S. U. C. S., Rubner, Y., Tomasi, C., & Guibas, L. J. (1998). The Earth mover's distance as a metric for image retrieval.

DJI, 2023. DJI Mavic Pro 2 Specifications. DJI. Available at:https://www.dji.com/global/mavic-2/info [Accessed July 4, 2023].

Duda, R. O., & Hart, P. E. (1972). Use of the Hough transformation to detect lines and curves in pictures. Communications of the ACM, 15(1), 11–15.

Gedraite, E. S., & Hadad, M. (2011, September). Investigation on the effect of a Gaussian Blur in image filtering and segmentation. In Proceedings ELMAR-2011 (pp. 393-396). IEEE.

Girshick, R. (2015). Fast r-cnn. In Proceedings of the IEEE international conference on computer vision (pp. 1440-1448)

Goodfellow, I., Bengio, Y., & Courville, A. (2016). Deep learning. MIT press.

Han, J., Yang, Z., Zhang, Q., Chen, C., Li, H., Lai, S., ... & Chen, R. (2019). A method of insulator faults detection in aerial images for high-voltage transmission lines inspection. Applied Sciences, 9(10), 2009.

He, K., Zhang, X., Ren, S., & Sun, J. (2016). Deep residual learning for image recognition. In Proceedings of the IEEE conference on computer vision and pattern recognition (pp. 770-778).

Hochreiter, S. (1998). The vanishing gradient problem during learning recurrent neural nets and problem solutions. International Journal of Uncertainty, Fuzziness and Knowledge-Based Systems, 6(02), 107-116.

Hosseini, M. M., Umunnakwe, A., Parvania, M., & Tasdizen, T. (2020). Intelligent damage classification and estimation in power distribution poles using unmanned aerial vehicles and convolutional neural networks. IEEE Transactions on Smart Grid, 11(4), 3325-3333.

Jafari, M., Hou, F., & Abdelkefi, A. (2020). Wind-induced vibration of structural cables. Nonlinear Dynamics, 100, 351-421.

Jain, A. K., Mao, J., & Mohiuddin, K. M. (1996). Artificial neural networks: A tutorial. Computer, 29(3), 31-44

Jenssen, R., & Roverso, D. (2019). Intelligent monitoring and inspection of power line components powered by UAVs and deep learning. IEEE Power and energy technology systems journal, 6(1), 11-21.

Jones, D. I., & Earp, G. K. (2001). Camera sightline pointing requirements for aerial inspection of overhead power lines. In Electric Power Systems Research (Vol. 57). www.elsevier.com/locate/epsr

Kanopoulos, N., Vasanthavada, N., & Baker, R. L. (1988). Design of an image edge detection filter using the Sobel operator. IEEE Journal of Solid-State Circuits, 23(2), 358–367.

Katrašnik, J., Pernuš, F., & Likar, B. (2010). A survey of mobile robots for distribution power line inspection. IEEE Transactions on Power Delivery, 25(1), 485–493. https://doi.org/10.1109/TPWRD.2009.2035427

Kim, T., Lee, Y., Sanyal, S., Woo, J., Choi, I. S., & Yi, J. (2020). Mechanism of corrosion in porcelain insulators and its effect on the lifetime. *Applied Sciences*, *10*(1), 423. https://doi.org/10.3390/app10010423

Kolb, D. A. (2014). Experiential learning: Experience as the Source of Learning and Development. FT Press.

Landi, A., Piaggi, P., Laurino, M., & Menicucci, D. (2010, November). Artificial neural networks for nonlinear regression and classification. In 2010 10th International Conference on Intelligent Systems Design and Applications (pp. 115-120). IEEE.

L, E. T., Moses, N. O., O, E. A., & Jonah, C. (2014). Network and Complex Systems Overview Of Losses and Solutions In Power Transmission Lines. 4(8). www.iiste.org

Li, F., Xin, J., Chen, T., Xin, L., Wei, Z., Li, Y., ... & Liao, H. (2020). An automatic detection method of bird's nest on transmission line tower based on faster_RCNN. IEEE Access, 8, 164214-164221.

Li, L., Gao, X., & Liu, W. (2021, December). On-line monitoring method of transmission tower tilt based on remote sensing satellite optical image and neural network. In 2021 11th International Conference on Power and Energy Systems (ICPES) (pp. 124-128). IEEE.

Li, Z., Bruggemann, T. S., Ford, J. J., Mejias, L., & Liu, Y. (2012). Toward automated power line corridor monitoring using advanced aircraft control and multisource feature fusion. Journal of Field Robotics, 29(1), 4-24.

Lin, T. Y., Dollár, P., Girshick, R., He, K., Hariharan, B., & Belongie, S. (2017). Feature pyramid networks for object detection. In Proceedings of the IEEE conference on computer vision and pattern recognition (pp. 2117-2125).

Lin, T. Y., Dollár, P., Girshick, R., He, K., Hariharan, B., & Belongie, S. (2017). Feature pyramid networks for object detection. In Proceedings of the IEEE conference on computer vision and pattern recognition (pp. 2117-2125).

Lin, T. Y., Goyal, P., Girshick, R., He, K., & Dollár, P. (2017). Focal loss for dense object detection. In Proceedings of the IEEE international conference on computer vision (pp. 2980-2988).

Liu, B., & Liu, B. (2011). Supervised learning. Web Data Mining: Exploring Hyperlinks, Contents, and Usage Data, 63-132.

Liu, W., Anguelov, D., Erhan, D., Szegedy, C., Reed, S., Fu, C. Y., & Berg, A. C. (2016). Ssd: Single shot multibox detector. In Computer Vision–ECCV 2016: 14th European Conference, Amsterdam, The Netherlands, October 11–14, 2016, Proceedings, Part I 14 (pp. 21-37). Springer International Publishing.

Liu, X., Miao, X., Jiang, H., & Chen, J. (2020). Review of data analysis in vision inspection of power lines with an in-depth discussion of deep learning technology. https://doi.org/10.1016/j.arcontrol.2020.09.002

Lloyd, S. (1982). Least squares quantization in PCM. IEEE transactions on information theory, 28(2), 129-137.

Malhara, S., & Vittal, V. (2009). Monitoring sag and tension of a tilted transmission line using geometric transformation. *IEEE Power & Energy Society General Meeting*. https://doi.org/10.1109/pes.2009.5275935

Matikainen, L., Lehtomäki, M., Ahokas, E., Hyyppä, J., Karjalainen, M., Jaakkola, A., ... & Heinonen, T. (2016). Remote sensing methods for power line corridor surveys. ISPRS Journal of Photogrammetry and Remote sensing, 119, 10-31.

Mohsan, S. A. H., Othman, N. Q. H., Li, Y., Alsharif, M. H., & Khan, M. A. (2023). Unmanned aerial vehicles (UAVs): Practical aspects, applications, open challenges, security issues, and future trends. Intelligent Service Robotics, 16(1), 109-137.

O'Shea, K., & Nash, R. (2015). An introduction to convolutional neural networks. arXiv preprint arXiv:1511.08458.

Poletaev, I. E., Pervunin, K. S., & Tokarev, M. P. (2016, October). Artificial neural network for bubbles pattern recognition on the images. In Journal of Physics: Conference Series (Vol. 754, No. 7, p. 072002). IOP Publishing.

R. Aracil, M. Ferre, M. Hernando, E. Pinto, and J. Sebastian, “Teler- obotic system for live-power line maintenance: Robtet,” Control Engi- neering Practice, vol. 10, no. 11, pp. 1271–1281, 2002.

Redmon, J., & Farhadi, A. (2018). Yolov3: An incremental improvement. arXiv preprint arXiv:1804.02767.

Ren, S., He, K., Girshick, R., & Sun, J. (2015). Faster r-cnn: Towards real-time object detection with region proposal networks. Advances in neural information processing systems, 28.

Russell, B. C., Torralba, A., Murphy, K. P., & Freeman, W. T. (2008). LabelMe: a database and web-based tool for image annotation. International journal of computer vision, 77, 157-173.

Sampedro, C., Martinez, C., Chauhan, A., & Campoy, P. (2014, July). A supervised approach to electric tower detection and classification for power line inspection. In 2014 International Joint Conference on Neural Networks (IJCNN) (pp. 1970-1977). IEEE.

Soille, P. (2000). Morphological image analysis: principles and applications. Sensor Review, 20(3). https://doi.org/10.1108/sr.2000.08720cae.001

Stewart, M., Martin, S., & Barrera, N. (2021). Unmanned aerial vehicles: fundamentals, components, mechanics, and regulations. Unmanned Aerial Vehicles, 1-70.

Surya Prasad, P., & Prabhakara Rao, B. (2016). Review on Machine Vision based Insulator Inspection Systems for Power Distribution System. Journal of Engineering Science and Technology Review, 9(5), 135–141. https://doi.org/10.25103/jestr.095.21

Tan, H. H., & Lim, K. H. (2019, June). Vanishing gradient mitigation with deep learning neural network optimization. In 2019 7th international conference on smart computing & communications (ICSCC) (pp. 1-4). IEEE.

Torre, V., & Poggio, T. A. (1986). On edge detection. IEEE Transactions on Pattern Analysis and Machine Intelligence, (2), 147-163.

Turkish Electricity Transmission Corporation (2023). Türkiye'de Elektrik İletimi Sayılarla İletim İstatistikleri. Retrieved from https://www.teias.gov.tr/sayilarla-elektrik-iletimi

UKEssays. (November 2018). Automated Power Pole Photography via Helicopters. Retrieved from https://www.ukessays.com/essays/engineering/automated-power-pole-photography-via-2357.php?vref=1

United States. (2010) U.S. Energy Information Administration EIA. United States. [Web Archive] Retrieved from the Library of Congress, https://www.eia.gov/energyexplained/electricity/

Varghese, A., Gubbi, J., Sharma, H., & Balamuralidhar, P. (2017, May). Power infrastructure monitoring and damage detection using drone captured images. In 2017 international joint conference on neural networks (IJCNN) (pp. 1681-1687). IEEE.

Von Gioi, R. G., Jakubowicz, J., Morel, J. M., & Randall, G. (2012). LSD: A line segment detector. Image Processing On Line, 2, 35-55

Yang, Y., Wang, M., Wang, X., Li, C., Shang, Z., & Zhao, L. (2022). A Novel Monocular Vision Technique for the Detection of Electric Transmission Tower Tilting Trend. Applied Sciences, 13(1), 407.

Yuan, Z., Tu, Y., Li, R., Zhang, F., Gong, B., & Wang, C. (2020). Review on the characteristics, heating sources and evolutionary processes of the operating composite insulators with abnormal temperature rise. CSEE Journal of Power and Energy Systems, 8(3), 910-921.

Zhang, W., Witharana, C., Li, W., Zhang, C., Li, X., & Parent, J. (2018). Using deep learning to identify utility poles with crossarms and estimate their locations from google street view images. Sensors, 18(8), 2484.

Zhao, K., Han, Q., Zhang, C. B., Xu, J., & Cheng, M. M. (2021). Deep hough transform for semantic line detection. IEEE Transactions on Pattern Analysis and Machine Intelligence, 44(9), 4793-4806.

Zhou, Z. H. (2016). Learnware: on the future of machine learning. *Frontiers Comput. Sci.*, *10*(4), 589-590.

W. Tong, J. Yuan, and B. Li, "Application of image processing in patrol inspection of overhead transmission line by helicopter," Power System Technology, vol. 34, no. 12, pp. 204–208, 2010

Wang, H., Cheng, L., Liao, R., Zhang, S., & Yang, L. (2019). Non-destructive testing method of micro-debonding defects in composite insulation based on high power ultrasonic. High Voltage, 4(3), 167-172.

Wang, H., Yang, G., Li, E., Tian, Y., Zhao, M., & Liang, Z. (2019, July). High-voltage power transmission tower detection based on faster R-CNN and YOLO-V3. In 2019 Chinese Control Conference (CCC) (pp. 8750-8755). IEEE.

Wang, S., Liu, Y., Qing, Y., Wang, C., Lan, T., & Yao, R. (2020). Detection of insulator defects with improved ResNeSt and region proposal network. IEEE Access, 8, 184841-184850.

Xue, J., & Su, B. (2017). Significant remote sensing vegetation indices: A review of developments and applications. Journal of sensors, 2017.